
Robust Linear Dueling Bandits with Post-serving Context under Unknown Delays and Adversarial Corruptions

Youngmin Oh¹

Abstract

We study linear dueling bandits in volatile environments characterized by the simultaneous presence of post-serving contexts, delayed feedback, and adversarial corruption. Feedback is subject to unknown stochastic or adversarial delays and a cumulative corruption budget \mathcal{C} . To address these challenges, we propose RCDP-UCB, which integrates a learned approximator that predicts post-serving contexts from pre-serving information. It further employs an adaptive weighting strategy that clips feature vectors to mitigate the impact of corrupted and delayed observations simultaneously. Under standard regularity conditions and a parametric post-serving mapping, we rigorously establish that our algorithm is delay-regime-agnostic, achieving a regret upper bound of $\tilde{O}(d(\sqrt{T} + \mathcal{C} + \mathcal{D}))$, where d is the total feature dimension and \mathcal{D} encapsulates the delay complexity. Crucially, our analysis reveals an additive cost structure between corruption and delay, avoiding the multiplicative degradation typical of prior works. We further establish lower bounds that nearly match our upper bounds up to a \sqrt{d} factor for adversarial delays in the absence of post-serving contexts.

1. Introduction

While the multi-armed bandit (MAB) framework successfully models various decision-making problems—ranging from recommendation systems to ad allocation (Lattimore & Szepesvári, 2020)—designing explicit real-valued reward functions often proves elusive in practice. Indeed, in many modern interactive systems, user feedback is inherently relative rather than absolute. For instance, a user may readily prefer Movie A over Movie B, yet find it difficult to assign a precise numerical score to either.

¹InfiniTree, Republic of Korea. Correspondence to: Youngmin Oh <youngmin0.oh@gmail.com>.

This reliance on relative feedback has become increasingly critical with the advent of Large Language Models (LLMs) (Guo et al., 2025). Reinforcement Learning from Human Feedback (RLHF) (Ouyang et al., 2022; Rafailov et al., 2023), one of the techniques for training LLMs, fundamentally relies on pairwise preference comparisons to align model outputs with human intent, demonstrating the pivotal role of preference-based learning in state-of-the-art AI systems (Guo et al., 2025; Achiam et al., 2023). This preference-based learning is elegantly formulated by the dueling bandits framework (Yue et al., 2012). To leverage side information for personalization in these complex environments, this framework has been further extended to the contextual setting (Dudík et al., 2015; Saha, 2021), bridging the gap between theoretical preference modeling and practical, high-dimensional applications.

However, existing contextual dueling bandit algorithms predominantly operate under the assumption that the utility of an arm is fully determined by the pre-serving context—features observable before an action is selected (e.g., user demographics, item metadata). This assumption fails to capture critical factors that are only revealed after the service is rendered, which we term post-serving contexts following Wang et al. (2024). For instance, in food delivery, the true enjoyment of a meal depends not only on the restaurant’s cuisine (pre-serving) but also on the actual delivery time and food temperature (post-serving). Similarly, in ride-sharing, a user’s satisfaction depends on the car type (pre-serving) as well as the cleanliness and driver conduct (post-serving). Ignoring these latent, post-hoc determinants can lead to suboptimal policy learning, as the learner fails to account for the full causal mechanism driving user preferences.

Compounding this challenge, real-world feedback is rarely instantaneous or pristine. Feedback often arrives with unknown stochastic or adversarial delays (Vernade et al., 2020; Lancewicki et al., 2023; Howson et al., 2023), and the observed outcomes may be subject to malicious corruption (Liu et al., 2024; Di et al., 2024). The interplay between latent post-serving contexts, delayed feedback, and adversarial corruption creates a hostile environment where standard regret minimization strategies typically fail.

Table 1. Comparison of cumulative regret upper bounds for various contextual bandit settings. We further omit sub-leading terms to highlight the dominant scaling (e.g., λ).

SETTING	CORRUPTION	DELAY	ALGORITHM	UPPER BOUND
LINEAR BANDITS	NO	NO	OFUL (ABBASI-YADKORI ET AL., 2011)	$\tilde{O}(d\sqrt{T})$
	YES	NO	CW-OFUL (HE ET AL., 2022)	$\tilde{O}(d\sqrt{T} + d\mathcal{C})$
	NO	STOCHASTIC	DELAYED-UCB (ZHOU ET AL., 2019)	$\tilde{O}(\sqrt{dT}(d + \mathbb{E}[\tau]))$
			OTFLINUCB* (VERNADE ET AL., 2020)	$\tilde{O}((d\sqrt{T} + md)/\tau_m)$
			GLB-UCB† (HOWSON ET AL., 2023)	$\tilde{O}(d\sqrt{T} + d^{3/2}\mathbb{E}[\tau])$
NO	ADVERSARIAL	ITO ET AL. (2020)	$\tilde{O}(\sqrt{d}(d + d_{\max})T)$	
GENERALIZED LINEAR BANDITS	NO	NO	GLM-UCB (FILIPPI ET AL., 2010)	$\tilde{O}(d\sqrt{T})$
	YES	NO	GADAOFUL (YU ET AL., 2025)	$\tilde{O}(d\sqrt{\sum_t \sigma_t^2} + d\mathcal{C})$
	YES	NO	YE ET AL. (2023)	$\tilde{O}(d\sqrt{T} + d\mathcal{C})$
	NO	STOCHASTIC	DELAYED-UCB (ZHOU ET AL., 2019)	$\tilde{O}(d\sqrt{T} + d\mathbb{E}[\tau]\sqrt{T})$
			GLB-UCB (HOWSON ET AL., 2023)	$\tilde{O}(d\sqrt{T} + d^{3/2}\mathbb{E}[\tau])$
LINEAR DUELING BANDITS	NO	NO	SAHA (2021); BENGS ET AL. (2022)	$\tilde{O}(d\sqrt{T})$
	YES	NO	RCDP (DI ET AL., 2024)	$\tilde{O}(d\sqrt{T} + d\mathcal{C})$
	YES	BOTH	RCDP-UCB (OURS)	$\tilde{O}(d(\sqrt{T} + \mathcal{C} + \mathcal{D}))$

d : feature dimension; T : time horizon; \mathcal{C} : total corruption budget; $\mathbb{E}[\tau]$: expected delay; d_{\max} : maximum delay; κ : lower bound of the link function derivative; σ_t^2 : variance at round t ; $\mathcal{D} = \max(\mu_\tau, \Lambda^{1/2})$, where μ_τ is the mean of the sub-Gaussian delay and Λ is the total adversarial delay budget; $\tau_m = \mathbb{P}(D \leq m)$ denotes the cumulative probability of the delay falling within window m .

Specifically, the uncertainty in mapping pre-serving to post-serving contexts introduces non-stationarity, while delays and corruption can severely skew the learner’s perception of utility. Solving this tripartite problem poses a substantial theoretical challenge, as the combined effect of these factors is fundamentally multiplicative rather than additive. Delays significantly reduce the effective sample size available for immediate updates, creating a data-scarce regime. This sparsity amplifies the statistical influence of adversarial corruptions: in the absence of abundant data, each observed feedback signal carries disproportionately high leverage. Consequently, an adversary can exert considerable bias by selectively corrupting these sparse observations, rendering the learning process highly sensitive to minor perturbations. Moreover, the learner must estimate a mapping from pre-serving to post-serving contexts using already-compromised and delayed feedback. This creates a vicious cycle: corrupted signals degrade the context predictor, which in turn magnifies estimation errors where delays have already starved the model of reliable data.

To surmount these intertwined challenges, we propose RCDP-UCB (Robust to Corruption, Delay, and Post-serving UCB), an algorithmic framework. To handle corrupted and delayed observations, we employ a weighted ridge regression estimator with an uncertainty-aware re-weighting mechanism. The intuition is as follows: observations that appear unreliable—either due to excessive delay or potential corruption—receive lower weight. This allows the learner to

gracefully degrade under attack rather than catastrophically fail. In our setting, post-serving contexts are revealed after the decision, forcing the learner to act under partial information. We construct a confidence ellipsoid that explicitly accounts for this additional variance, enabling principled optimism over both the unknown preference parameters and the unobserved features.

A key feature of our approach is that it does not require prior knowledge of the specific delay mechanism type (stochastic vs. adversarial). While the aggregate magnitude of the corruption and delay budgets is utilized for theoretical tuning of the clipping threshold α , the algorithm adapts efficiently without needing to detect or classify the source of the delay.

We establish the first regret guarantees for linear dueling bandits within this unified tripartite setting. Under standard regularity conditions and a parametric post-serving mapping, we achieve a regret bound of: $\tilde{O}\left(d\left(\sqrt{T} + \mathcal{C} + \mathcal{D}\right)\right)$, where d denotes the feature dimension, T is the time horizon, and \mathcal{C} represents the cumulative corruption budget. Notably, our framework provides best-of-both-worlds guarantees in terms of delay regimes for the delay complexity \mathcal{D} , which adaptively scales as $\Lambda^{1/2}$ for an adversarial delay budget Λ , or as the mean delay μ_τ for sub-Gaussian distributions. Each component of the bound admits a transparent interpretation: $d\sqrt{T}$ represents the fundamental cost of learning, $d\mathcal{D}$ captures the penalty incurred by delayed feedback, and $d\mathcal{C}$ reflects the impact of adversarial corruptions.

To certify the optimality of our results, we derive a lower bound of $\Omega(\sqrt{dT} + d\mathcal{C} + \mathcal{D}')$ in the absence of post-serving contexts, where $\mathcal{D}' = \max\{\sqrt{d\Lambda}, d\mu_\tau\}$. This confirms that the overhead introduced by delays and corruptions is information-theoretically unavoidable, and that RCDP-UCB achieves this limit with near-optimal efficiency up to a \sqrt{d} factor for adversarial delays. To the best of our knowledge, this work is the first to simultaneously address the joint challenges of adversarial corruptions and delayed feedback within the contextual dueling bandit framework.

Our primary contributions are summarized as follows:

- **Unified Analytical Framework:** We formalize a linear dueling bandit framework tailored for volatile environments, providing a comprehensive treatment of three critical practical challenges: post-serving contexts, unknown observation delays, and adversarial corruptions.
- **Unified & Delay-Agnostic Mechanism:** We propose RCDP-UCB, which employs a novel adaptive weighting strategy anchored to the full information geometry. This design renders our algorithm **delay-regime-agnostic**, requiring no prior knowledge of whether delays are stochastic or adversarial. Crucially, this mechanism structurally decouples corruption from delay, achieving an **additive** $\mathcal{C} + \mathcal{D}$ cost rather than a multiplicative one.
- **Regret Analysis:** We prove a regret upper bound of $\tilde{\mathcal{O}}(d(\sqrt{T} + \mathcal{C} + \mathcal{D}))$, matching our lower bound up to a \sqrt{d} factor in the adversarial delay regime.

2. Related Work

Linear Contextual Dueling Bandits. Linear utility functions in CDBs have been extensively studied (Bengs et al., 2022; Saha, 2021; Di et al., 2023; Li et al., 2024). Bengs et al. (2022) and Saha (2021) established UCB-based regret bounds of $\tilde{\mathcal{O}}(d\sqrt{T})$ and $\tilde{\mathcal{O}}(\sqrt{dT})$, matching the lower bounds identified by Saha (2021). Alternative approaches include the variance-aware action-elimination method by Di et al. (2023) and the Thompson Sampling-based algorithm by Li et al. (2024), which also achieves $\mathcal{O}(d\sqrt{T})$ regret.

Robustness to Adversarial Corruption. Addressing the vulnerability of bandit algorithms to data poisoning remains a pivotal challenge. A fundamental distinction exists between action-independent (weak) and action-dependent (strong) corruption. In the context of linear bandits, He et al. (2022) and Liu et al. (2024) established the minimax regret bounds under corruption. For Generalized Linear Bandits (GLBs), Yu et al. (2025) introduced GAdaOFUL, a variance-aware algorithm utilizing adaptive Huber regression. More

recently, Ye et al. (2023) proposed CR-GLM-UW, which leverages uncertainty weighting to achieve robust performance without prior knowledge of the corruption level. In the realm of Dueling Bandits, while earlier works like Agarwal et al. (2021) addressed general robustness, Di et al. (2024) recently developed RCDB, achieving nearly optimal regret bounds in the presence of strong corruptions.

Delayed Feedback Mechanisms. Delays in outcome observation significantly complicate the regret landscape. For stochastic delays in linear bandits, Zhou et al. (2019) provided foundational upper bounds, which Vernade et al. (2020) extended to scenarios with censored feedback (OTFLinUCB). In the GLB setting, Howson et al. (2023) demonstrated that with appropriate optimism, the regret penalty remains additive with respect to the expected delay. Regarding adversarial delays, Ito et al. (2020) derived regret bounds dependent on the maximum delay d_{\max} . Despite these advances, the intersection of heavy-tailed delays and adversarial corruption—particularly in the preference-based setting—remains largely unexplored, a gap our work aims to bridge.

Post-Serving Contexts and Partial Observability. When valuable contextual information is only observable after arm selection, standard contextual bandit algorithms may suffer from model misspecification. Wang et al. (2024) introduced the framework of contextual bandits with post-serving contexts, proposing the poLinUCB algorithm that achieves regret $\tilde{\mathcal{O}}(T^{1-\alpha}d_u^\alpha + d_u\sqrt{TK})$, where $\alpha \in [0, 1/2]$ captures the learnability of the pre- to post-context mapping function. Central to their analysis is a robustified Elliptical Potential Lemma (EPL) that accommodates noise in observed features. Earlier work by Wang et al. (2016) studied hidden contexts under strong initialization assumptions, while subsequent research explored noisy or unobservable contexts through online prediction from context histories (Qi et al., 2018; Yang et al., 2020; Yang & Ren, 2021; Zhu & Kveton, 2022). Park & Faradonbeh (2021) further analyzed the Thompson Sampling algorithm under partial observability constraints.

3. Problem Formulation

Basic Setup with Post-serving Contexts. We consider a contextual dueling bandit problem over a finite horizon T with a finite K arms. In each round $t \in [T]$, the environment provides a pre-serving context set $\mathcal{X}_t = \{x_{t,1}, \dots, x_{t,K}\} \subset \mathbb{R}^{d_x}$. Then the learner selects a pair of arms $(a_t, b_t) \in [K] \times [K]$. Following the selection, the learner observes the associated post-serving contexts $y_{t,a_t}, y_{t,b_t} \in \mathbb{R}^{d_y}$ as in Wang et al. (2024). The complete feature representation for an arm k is defined as the concatenation $z_{t,k} = (x_{t,k}, y_{t,k}) \in \mathbb{R}^d$, where $d = d_x + d_y$. We as-

sume that there is a learnable mapping $\phi_*(\cdot) : \mathbb{R}^{d_x} \rightarrow \mathbb{R}^{d_y}$ such that $y_{t,k} = \phi_*(x_{t,k}) + \epsilon_{t,k}$ where $\epsilon_{t,k}$ is a zero-mean noise vector, i.e., $\phi_*(x_{t,k}) = \mathbb{E}[y_{t,k} | x_{t,k}]$. We adopt a linear utility model with an unknown parameter $\Theta_* \in \mathbb{R}^d$, where the utility of arm k at round t is given by $u_{t,k} = \langle \Theta_*, z_{t,k} \rangle$ for $k \in [K]$. The preference probability between arms a_t and b_t is governed by a link function $g : \mathbb{R} \rightarrow [0, 1]$. Specifically, the binary outcome $l_t \in \{0, 1\}$ satisfies $\mathbb{E}[l_t | a_t, b_t] = g(\langle \Theta_*, z_{t,a_t} - z_{t,b_t} \rangle)$. A prominent example is the logistic link function $g(x) = \frac{1}{1 + \exp(-x)}$, corresponding to the Bradley-Terry-Luce (BTL) model (Hunter, 2004; Luce, 2005).

Feedback Delay. A distinguishing feature of our setting is that the learner operates without prior knowledge of whether the delay sequence $\{\tau_t\}_{t=1}^T$ is governed by a stochastic process or determined by an adversary. The delay regime is fixed throughout the entire horizon but remains unknown to the learner. We consider two canonical settings:

1. **Stochastic Delays.** The delays $\{\tau_t\}_{t=1}^T$ are independent σ^2 -sub-Gaussian random variables with mean μ_τ . That is, for all $n \in \mathbb{R}$, $\mathbb{E}[\exp(n(\tau_t - \mu_\tau))] \leq \exp\left(\frac{n^2 \sigma^2}{2}\right)$ as in Howson et al. (2023).
2. **Adversarial Delays.** An adaptive adversary selects the delay sequence subject to a cumulative budget constraint: $\sum_{t=1}^T \tau_t \leq \Lambda$. The adversary may choose τ_t based on $\mathcal{H}_{t-1} = \{s \in [t-1] : s + \tau_s < t\}$, consisting of all rounds whose feedback has arrived.

Feedback Corruption. Before the outcome is revealed to the learner, an adversary may corrupt the true signal l_t to produce a corrupted observation $\gamma_t \in \{0, 1\}$. The adversary is constrained by a total corruption budget C : $\sum_{t=1}^T |l_t - \gamma_t| \leq C$. Accordingly, we let o_t be the observed outcome to the learner, which is unknown whether $o_t = l_t$ or not.

Regret Definition. The learner's objective is to minimize the cumulative average regret R_T . Let $k_t^* = \arg \max_{k \in [K]} \langle \Theta_*, z_{t,k} \rangle$ be the optimal arm at round t . The instantaneous regret r_t is defined as the utility gap between the optimal arm and the selected pair (Saha, 2021):

$$r_t = \frac{1}{2} (\langle \Theta_*, z_{t,k_t^*} - z_{t,a_t} \rangle + \langle \Theta_*, z_{t,k_t^*} - z_{t,b_t} \rangle).$$

The total cumulative regret is thus $R_T = \sum_{t=1}^T r_t$. The learner must achieve sublinear regret while remaining agnostic to the specific delay regime and the presence of corruption.

4. RCDP-UCB

To establish the theoretical guarantees for our proposed algorithm, we introduce the following structural and statistical assumptions. These are standard in the literature on generalized linear bandits and contextual dueling bandits with auxiliary information (Pike-Burke et al., 2018; Di et al., 2024; Bengs et al., 2022; Di et al., 2023).

Assumption 4.1. The link function $g : \mathbb{R} \rightarrow [0, 1]$ is continuously differentiable, and there exists a constant $\kappa > 0$ such that its derivative satisfies $\dot{g}(s) \geq \kappa$ for all s in the domain of interest.

Assumption 4.2. The true underlying parameter $\Theta_* \in \mathbb{R}^d$ is contained within a ball of radius M , i.e., $\|\Theta_*\|_2 \leq M$ for some known constant $M > 0$.

Assumption 4.3 (\mathcal{L}_2 -Consistency and Convergence Rate). Let \mathcal{D} be a probability distribution over $\mathcal{X} \times \mathcal{Y}$. We assume the existence of an estimation algorithm that, given a dataset $S = \{(x_s, y_s)\}_{s=1}^t$ sampled i.i.d. from \mathcal{D} , produces an estimator $\hat{\phi}_t : \mathcal{X} \rightarrow \mathbb{R}^{d_y}$. Furthermore, we assume that there exist constants $C_0 > 0$ and $\nu \in (0, 1/2]$ such that for any $\delta \in (0, 1)$, the estimator $\hat{\phi}_t$ satisfies the following uniform error bound with probability at least $1 - \delta$:

$$\sup_{x \in \mathcal{X}} \|\hat{\phi}_t(x) - \phi_*(x)\|_2 \leq C_0 \frac{\sqrt{d_x}}{t^\nu} \log(t/\delta),$$

where ϕ_* is the underlying ground-truth function.

Remark 4.1 (Spectral and Smoothness Interpretations). Assumption 4.3 encapsulates various functional regimes:

- **Parametric Linear Case:** If $\phi_*(x) = \Phi^\top x$, then $\nu = 1/2$ is achievable via ordinary least squares or ridge regression (Abbasi-Yadkori et al., 2011).
- **Non-parametric Hölder Continuity:** For $\phi_* \in \mathcal{H}_\beta(\mathcal{X})$, the minimax optimal rate is $\nu = \beta/(2\beta + d_x)$, reflecting the curse of dimensionality (Tsybakov, 2008).
- **Reproducing Kernel Hilbert Spaces (RKHS):** For functions with bounded norm in an RKHS, $\nu = 1/2$ can be recovered under standard regularity conditions (Srinivas et al., 2012).

We assume the boundedness of contexts in the L_2 norm for the sake of simplicity:

Assumption 4.4. The joint feature vectors are bounded within a ball of radius $1/2$, i.e., $\|z_{t,k}\|_2 \leq 1/2$ for all $t \in [T]$ and $k \in [K]$. Consequently, the pairwise feature differences satisfy $\|\Delta z_{t,k_1,k_2}\|_2 \leq 1$, where $\Delta z_{t,k_1,k_2} := z_{t,k_1} - z_{t,k_2}$.

We define the following weighted design matrix to facilitate

our analysis with weights $\{\omega_s\}_{s=1}^t$:

$$\tilde{V}_t = \lambda I + \kappa \sum_{s=1}^t \omega_s \Delta z_s \Delta z_s^\top, \quad (1)$$

$$\tilde{W}_t = \lambda I + \kappa \sum_{s=1}^t \mathbb{I}\{s + \tau_s \leq t\} \omega_s \Delta z_s \Delta z_s^\top, \quad (2)$$

with $\Delta z_s = \Delta z_{s,a_s,b_s}$, where a_s and b_s are chosen arms at round s . We estimate the unknown parameter $\Theta_* \in \mathbb{R}^{d_x+d_y}$ by minimizing the weighted regularized negative log-likelihood, which corresponds to the Maximum Likelihood Estimation (MLE) with an ℓ_2 -regularizer:

$$\mathcal{L}_t(\Theta) = \frac{\lambda}{2} \|\Theta\|_2^2 - \sum_{s \in \mathcal{H}_{t-1}} \omega_s \log g((-1)^{1-o_s} \langle \Theta, \Delta z_s \rangle),$$

where $\Delta z_s = \Delta z_{s,a_s,b_s}$, and $\omega_s > 0$ is the weight for sample s . The estimator Θ_t is obtained as:

$$\Theta_t = \underset{\Theta \in \mathbb{R}^{d_x+d_y}}{\operatorname{argmin}} \mathcal{L}_t(\Theta). \quad (3)$$

Assuming g belongs to a set of exponential family distributions, the following estimating equation is obtained (Bengs et al., 2022):

$$\lambda \Theta_t + \sum_{s \in \mathcal{H}_{t-1}} \omega_s (g(\Theta_t^\top \Delta z_s) - o_s) \Delta z_s = 0.$$

To simultaneously mitigate the impact of adversarial corruption and stabilize the bias induced by delayed feedback, we propose the following adaptive weighting scheme. Let $\alpha > 0$ serve as a tuning parameter for robustness. We define the weight ω_s for the s -th sample as:

$$\omega_s = \min \left(1, \frac{\alpha}{\|\Delta z_s\|_{\tilde{V}_{s-1}^{-1}}} \right). \quad (4)$$

Geometrically, this weighting enforces the soft constraint $\|\sqrt{\omega_s} \Delta z_s\|_{\tilde{V}_{s-1}^{-1}} \leq \alpha$. It serves as a unified mechanism mitigating both adversarial corruptions and delay-induced bias. Note that while Di et al. (2024) utilized this strategy exclusively for robustness against corruption, our work establishes it as a unified mechanism that simultaneously counteracts both adversarial corruption and delayed feedback, with $\alpha = \sqrt{d}/(\mathcal{C} + \mathcal{D})$ tuned to achieve sublinear regret.

Furthermore, we let $\hat{\phi}_t$ be an estimator of ϕ_* at round t . Then we propose the following strategy RCDP-UCB: at each round t ,

$$a_t = \arg \max_{k \in [K]} \langle \Theta_{t-1}, \hat{z}_{t,k} \rangle, \quad (5)$$

$$b_t = \arg \max_{k \in [K]} \langle \Theta_{t-1}, \hat{z}_{t,k} \rangle + c_t \|\Delta \hat{z}_{t,k,a_t}\|_{\tilde{V}_{t-1}^{-1}}. \quad (6)$$

where $\hat{z}_{t,k} = (x_{t,k}, \hat{y}_{t,k})$ with $\hat{y}_{t,k} = \hat{\phi}_t(x_{t,k})$ and $\Delta z_{t,k,k'} := \hat{z}_{t,k} - \hat{z}_{t,k'}$ for $k, k' \in [K]$. Note that a learner cannot observe the post-serving contexts, so the learner estimates $\hat{y}_{t,k}$ of $y_{t,k}$ by utilizing $\hat{\phi}_t$. The value c_t will be specified later when analyzing the regret analysis. The full procedure is summarized in Algorithm 1.

Algorithm 1 RCDP-UCB

Input: Horizon T , dimension $d = d_x + d_y$, regularization λ , robustness parameter α , design matrix $\tilde{V}_0 = \lambda I$, $\tilde{W}_0 = \lambda I$, estimator $\Theta_0 = 0$, exploration parameter c_t . Initialize replay buffer $\mathcal{D} = \emptyset$, neural approximator $\hat{\phi}$.

for $t = 1$ **to** T **do**

1. Context Generation & Prediction:

Receive pre-serving contexts $\mathcal{X}_t = \{x_{t,k}\}_{k=1}^K$.

Form estimated features: $\hat{z}_{t,k} \leftarrow (x_{t,k}, \hat{y}_{t,k})$ where $\hat{y}_{t,k} \leftarrow \hat{\phi}_{t-1}(x_{t,k})$ for all $k \in [K]$.

2. Arm Selection & Execution:

Select pair (a_t, b_t) based on $\hat{z}_{t,k}$ using Equations (5) and (6).

Plays pair (a_t, b_t) and observe post-serving contexts

y_{t,a_t}, y_{t,b_t} .

Add (x_{t,a_t}, y_{t,a_t}) and (x_{t,b_t}, y_{t,b_t}) to \mathcal{D} .

3. Feedback Processing (Delayed Outcomes):

Update history $\mathcal{H}_t \leftarrow \{s \in [t] : s + \tau_s \leq t\}$.

Calculate weight $\omega_t \leftarrow \min(1, \alpha / \|\Delta z_t\|_{\tilde{V}_{t-1}^{-1}})$.

Update $\tilde{V}_t \leftarrow \tilde{V}_{t-1} + \kappa \omega_t \Delta z_t \Delta z_t^\top$.

for $s \in \mathcal{H}_t \setminus \mathcal{H}_{t-1}$ (newly arrived outcomes) **do**

Observe outcome o_s .

Update $\tilde{W}_s \leftarrow \tilde{W}_{s-1} + \kappa \omega_s \Delta z_s \Delta z_s^\top$.

end for

4. Model Updates:

Update $\hat{\phi}_t$ by training on \mathcal{D} .

Update Θ_t by minimizing weighted loss \mathcal{L}_t using available outcomes.

end for

Our algorithm, RCDP-UCB, employs \tilde{V}_t for both arm selection and robust weight calculation, rather than the observed matrix \tilde{W}_t . This approach enforces optimism in the face of scheduled uncertainty, effectively preventing redundant exploration in delayed settings and ensuring the selection strategy is consistent with the robustness mechanism. While exploration and weighting leverage this optimistic \tilde{V}_t , parameter estimation (Θ_t) remains strictly grounded in realized feedback via \tilde{W}_t , ensuring statistical validity.

5. Regret Analysis

A fundamental theoretical bottleneck in this regime arises from the multiplicative interplay between feedback latency and adversarial corruption, a challenge further exacerbated by post-serving contexts. Conventional analytical frame-

works typically decompose the weighted norm associated with the observed Gram matrix \widetilde{W}_t as follows $\|\Delta z_s\|_{\widetilde{W}_t^{-1}} \lesssim \|\Delta z_s\|_{\widetilde{V}_t^{-1}} + \|\Delta z_s\|_{\widetilde{M}_t^{-1}}$, where \widetilde{M}_t represents the adjustment matrix accounting for delayed observations. Following Howson et al. (2023), the delay adjustment satisfies $\|\Delta z_s\|_{\widetilde{M}_t^{-1}} \leq C(\tau_t)\|\Delta z_s\|_{\widetilde{V}_t^{-1}}^2$, where $C(\tau_t)$ scales with the cumulative delay. This interaction causes the corruption-induced bias to become multiplicatively coupled with the delay factor, yielding an unfavorable $\mathcal{O}(\mathcal{CD})$ term on the right-hand side of the regret bound.

Accordingly, we exploit a critical information asymmetry: while outcomes are subject to stochastic latency, the contexts (covariates) are revealed instantaneously upon action selection. Leveraging this, we propose anchoring our weighting mechanism to the full information geometry \widetilde{V}_t —constructed from the entire chronological sequence of contexts—rather than the partial, delay-dependent geometry \widetilde{W}_t . This methodological shift enables a strictly tighter regret decomposition through the following mechanisms:

1. **Statistical Leverage Stability:** By evaluating the statistical leverage scores of each sample relative to the global information manifold \widetilde{V}_{s-1} , we ensure that the importance weights defined in Equation (4) are determined a priori—at the moment of action selection. This design renders the estimation process invariant to adversarial manipulations of outcome arrival times, as the weighting mechanism is entirely decoupled from the delay sequence $\{\tau_t\}_{t=1}^T$.
2. **Structural Norm Decoupling:** The core utility of the \widetilde{V}_{t-1}^{-1} -norm is its ability to facilitate an additive error structure, allowing corruption and delay-induced errors to be bounded independently. This is achieved by partitioning the historical samples $\{1, \dots, t-1\}$ into three disjoint categories based on their observational status:

$$[t-1] = \underbrace{\mathcal{A}_t \cap \mathcal{E}^c}_{\text{arrived \& clean}} \sqcup \underbrace{\mathcal{A}_t \cap \mathcal{E}}_{\text{arrived \& corrupted}} \sqcup \underbrace{\mathcal{A}_t^c}_{\text{pending feedback}},$$

where $\mathcal{A}_t = \{s : s + \tau_s < t\}$ denotes the set of rounds whose feedback has arrived, and $\mathcal{E} = \{s : c_s = 1\}$ denotes the set of corrupted rounds.

By the approach above, we obtain the following concentration inequality estimation:

Lemma 5.1 (Estimation Error Bound). *Suppose that Assumption 4.1–Assumption 4.4 are satisfied. Let Θ_* denote the true parameter and Θ_t be the estimator satisfying Equation (3). Assume the link function satisfies $\dot{g}(x) \geq \kappa > 0$. Then, for any $\delta \in (0, 1)$, the following inequality holds with probability at least $1 - \delta$:*

$$\|\Theta_t - \Theta_*\|_{\widetilde{W}_{t-1}} \leq \|\Theta_t - \Theta_*\|_{\widetilde{V}_{t-1}} \leq \beta_t, \quad (7)$$

where the confidence radius β_t is defined as

$$\beta_t = \frac{1}{2} \sqrt{d \log \left(\frac{1 + t/(d\lambda)}{\delta} \right)} + \sqrt{\lambda} M + \alpha \mathcal{C} + \alpha \mathcal{D}$$

with $\mathcal{D} = \max(\Lambda^{1/2}, \mu_\tau)$.

The lemma above says that

$$(\text{Estimation Error}) \leq \underbrace{\mathcal{O}(\sqrt{d})}_{\text{statistical}} + \underbrace{\mathcal{O}(\mathcal{C}\alpha)}_{\text{corruption}} + \underbrace{\mathcal{O}(\mathcal{D}\alpha)}_{\text{delay}}.$$

Using Lemma 5.1, we obtain the following regret upper bounds.

Theorem 5.2 (Regret Upper Bound). *Suppose the conditions of Lemma 5.1 hold. By setting the exploration width $c_t = 2\beta_t$ and the parameter*

$$\alpha = \frac{\sqrt{d}}{\mathcal{C} + \mathcal{D}}, \quad (8)$$

the cumulative regret R_T satisfies

$$R_T = \widetilde{\mathcal{O}}(A_T + B_T),$$

omitting sub-leading terms additionally to highlight the dominant scaling, where $A_T = d \left(\sqrt{T} + \mathcal{C} + \mathcal{D} \right)$, $B_T = T^{1-\nu} d_x^\nu (1 + \sqrt{d})$.

Proof Sketch. The proof relies on a novel information-geometric decoupling that effectively separates estimation uncertainty from the regret decomposition. We distinguish between three feature variants: the estimated features $\Delta \widehat{z}_t$ used for selection, the observed noisy features Δz_t used for weighting, and the *noise-free latent ground-truth* Δz_t^* (where $z_{t,k}^* := (x_{t,k}, \phi_*(x_{t,k}))$).

Step 1: Robust Confidence Bounds via Bias-Variance Trade-off. By invoking Lemma 5.1, we establish that the estimation error is bounded by $\beta_t = \widetilde{\mathcal{O}}(\sqrt{d} + (\mathcal{C} + \mathcal{D})\alpha)$. Here, the term $(\mathcal{C} + \mathcal{D})\alpha$ quantifies the bias induced by adversarial corruption and invisible delayed feedback. We select the clipping threshold $\alpha = \sqrt{d}/(\mathcal{C} + \mathcal{D})$ to balance this bias against the variance, thereby yielding a dimension-dependent confidence radius of $\beta_t = \widetilde{\mathcal{O}}(\sqrt{d})$.

Step 2: Regret Decomposition and Approximation Control. Under the principle of optimism with exploration width $c_t = 2\beta_t$, the instantaneous regret is dominated by the uncertainty of the *selected* estimator: $r_t \lesssim \beta_t \|\Delta \widehat{z}_t\|_{\widetilde{V}_{t-1}^{-1}}$. By applying the triangle inequality and the learnability assumption (Assumption 4.3), we decompose this into the latent truth and the approximation error:

$$\|\Delta \widehat{z}_t\|_{\widetilde{V}_{t-1}^{-1}} \leq \|\Delta z_t^*\|_{\widetilde{V}_{t-1}^{-1}} + \|\Delta \widehat{z}_t - \Delta z_t^*\|_{\widetilde{V}_{t-1}^{-1}}.$$

The approximation error term accumulates to a sublinear order of $\tilde{\mathcal{O}}(T^{1-a})$, reducing the problem to bounding the cumulative elliptic potential of the latent features $\sum_{t=1}^T \|\Delta z_t^*\|_{\tilde{V}_{t-1}^{-1}}$.

Step 3: Weighted Analysis. Partitioning based on weights ω_t (derived from observed Δz_t), the unclipped regime sums to $\tilde{\mathcal{O}}(\sqrt{dT})$. In the clipped regime ($\|\Delta z_t\|_{\tilde{V}_{t-1}^{-1}} > \alpha$), using $\|\Delta z_t^*\| \approx \|\Delta z_t\|$, the contribution scales as $\alpha^{-1} \sum \omega_t \|\Delta z_t\|_{\tilde{V}_{t-1}^{-1}}^2 = \tilde{\mathcal{O}}(\alpha^{-1}d)$. Substituting α recovers $\tilde{\mathcal{O}}(d(\mathcal{C} + \mathcal{D}))$. \square

Furthermore, we establish lower bounds by establishing worst case instances, respectively.

Theorem 5.3 (Minimax Lower Bound). *Assume the absence of post-serving contexts. For any dimension d , corruption budget \mathcal{C} , horizon T , adversarial delay budget Λ , and mean stochastic delay μ_τ satisfying the conditions $T \geq \max\{\frac{4d^2}{25}, d\mathcal{C}\}$, $\Lambda \leq T^2$, and $\mu_\tau < T$, and for any algorithm \mathcal{A} , there exists an instance \mathcal{I} such that the expected regret is lower bounded by:*

$$\mathbb{E}[R_T(\mathcal{A}; \mathcal{I})] \geq \Omega\left(\frac{d\sqrt{T} + d\mathcal{C} + \mathcal{D}'}{\kappa}\right),$$

omitting sub-leading terms additionally to highlight the dominant scaling, where $\mathcal{D}' := \max\{\sqrt{d\Lambda}, d\mu_\tau\}$.

Remark 5.4 (Order-wise Optimality with $\nu = 1/2$). By setting $\nu = 1/2$, the regret upper bound in Theorem 5.2 can be simplified to: $R_T = \tilde{\mathcal{O}}\left(d\left(\sqrt{T} + \mathcal{C} + \max(\Lambda^{1/2}, \mu_\tau)\right)\right)$.

Neglecting the multiplicative factor of \sqrt{d} for adversarial delays, this result of R_T for $\nu = 1/2$ is remarkably consistent with the lower bounds established in Theorem 5.3. Both the upper and lower bounds exhibit a matching dependence on the primary parameters: the square-root of the time horizon \sqrt{T} , the linear corruption budget \mathcal{C} , and the respective delay budgets $\sqrt{\Lambda}$ and μ_τ . This alignment confirms the fundamental additive costs incurred by adversarial corruption and delayed feedback.

The rigorous justifications for Lemma 5.1 (Section A), Theorem 5.2 (Section B), and Theorem 5.3 (Section C) are provided to the supplementary material.

6. Experimental Results

We evaluate RCDP-UCB across synthetic environments simulating the interplay of latent post-serving dynamics, feedback corruption, and observation delays.

6.1. Experimental Setup

We consider a contextual dueling bandit problem with $d_x = 10$ and $K = 10$ arms. Pre-serving contexts are

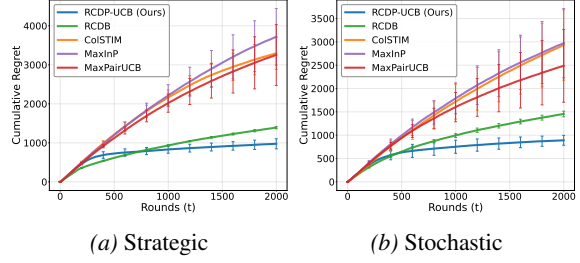


Figure 1. Performance comparison without post-serving contexts, i.e., the linear setting ($\mathcal{C} = 25$, $\Lambda = 10^4$, $\mu_\tau = 100$, $\sigma = 10$; 5 runs). RCDP-UCB consistently outperforms RCDB, demonstrating the robustness of our unified weighting mechanism.

sampled uniformly from $[-\pi, \pi]^{d_x}$. We employ three non-linear mappings $\phi_* : \mathbb{R}^{d_x} \rightarrow \mathbb{R}^{d_y}$: (i) Polynomial: $y_{t,k} \propto [x_{t,k}^2, \sqrt{|x_{t,k}|}]^\top$; (ii) Sinusoidal: $y_{t,k} \propto [\cos(x_{t,k}), \sin(x_{t,k})]^\top$; and (iii) Absolute: $y_{t,k} = |x_{t,k}|$.

The unknown mapping ϕ_* is approximated using a Multi-Layer Perceptron (MLP) $\hat{\phi}_t$ comprising two hidden layers (64 units each) with ReLU activations. The network is updated for 2 epochs per round using the Adam optimizer with a learning rate of 10^{-3} , utilizing an accumulated replay buffer of observed (x, y) pairs. We fix the regularization parameter $\lambda = 1.0$. We use the BTL model (Hunter, 2004; Luce, 2005) as the link function g . Detailed hyperparameter configurations are provided in Section D.

We investigate two delay regimes: (i) Stochastic Delay ($\tau_t \sim \mathcal{N}(\mu_\tau, \sigma^2)$) and (ii) Strategic Delay (adversarial starvation attack). We evaluate robustness under a prioritized interference protocol where the adversary favors strategic outcome corruption over delay. Subject to budget \mathcal{C} , corruption yields immediate falsified feedback, whereas delays affect only uncorrupted outcomes. This prioritization models a strategic adversary aiming to maximize the disruptive efficacy of the attack under the premise that direct outcome falsification impedes convergence more severely.

6.2. Baselines

We benchmark RCDP-UCB against state-of-the-art dueling bandit algorithms. To ensure a fair comparison, all baselines are provided with the observable pre-serving contexts \mathcal{X}_t . The baselines include: (i) **RCDB** (Di et al., 2024), a robust method utilizing weighted MLE; (ii) **ColSTIM** (Bengs et al., 2022), a randomized soft-elimination strategy; (iii) **MaxInP** (Saha, 2021), an approach based on maximizing information gain; (iv) **MaxPairUCB** (Di et al., 2023), a strategy comparing the two arms with the highest upper confidence bounds. In this section, we fix the aggregate error budget at $\mathcal{C} + \mathcal{D} = 125$, with a corruption budget of $\mathcal{C} = 25$. Accordingly, for both RCDP-UCB and RCDB, the robustness parameter α is pre-calibrated based on the

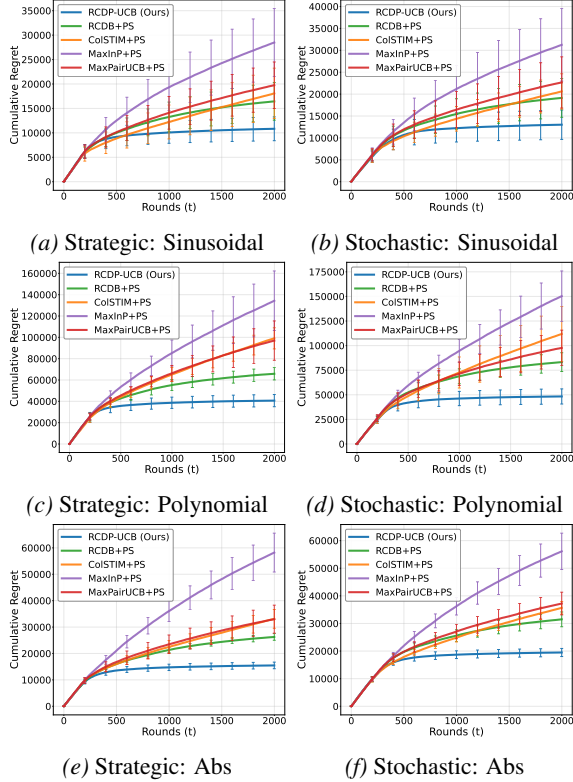


Figure 2. Cumulative regret with learned post-serving contexts ($\mathcal{C} = 25$, $\Lambda = 10^4$, $\mathcal{N}(100, 10^2)$). Averaged over 5 runs, RCDP-UCB consistently outperforms baselines, demonstrating superior robustness in latent environments.

theoretical results of each respective work.

6.3. Empirical Analysis

Efficacy of Adaptive Weighting. Figure 1 isolates the impact of our weighting strategy by comparing RCDP-UCB with baselines in a setting without post-serving contexts (i.e., a standard linear dueling problem). RCDP-UCB generalizes the RCDB framework by incorporating a unified budget $\mathcal{C} + \mathcal{D}$ into the weight calculation (Equation (4)). RCDP-UCB consistently outperforms baselines across all delay settings. This confirms that down-weighting observations by Equation (4) effectively mitigates instability from both corruption and delay.

Robustness in Latent Post-Serving Environments. Figure 2 presents the cumulative regret in environments with non-linear post-serving mappings. Here, all algorithms (including baselines) are augmented to learn ϕ_* . RCDP-UCB achieves the lowest cumulative regret across all tasks (Absolute, Polynomial, Sinusoidal) independently of delay regimes. This demonstrates that our algorithm successfully leverages predicted post-serving contexts while neutralizing the adverse effects of delayed and corrupted feedback.

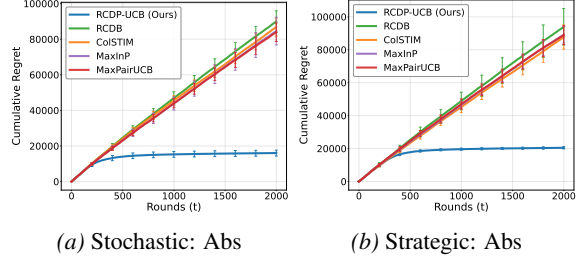


Figure 3. Cumulative regret where only RCDP-UCB exploits the learned mapping ϕ_* , while baselines are restricted to pre-serving contexts ($\mathcal{C} = 25$, $\Lambda = 10^4$, $\mathcal{N}(100, 10^2)$). Averaged over 5 runs, RCDP-UCB demonstrates superior performance relative to the baselines.

Impact of Post-Serving Context Awareness. Figure 3 further investigates the scenario where only RCDP-UCB learns and utilizes the post-serving mapping ϕ_* , while baselines rely solely on pre-serving contexts. As expected, RCDP-UCB typically outperforms the baselines. This highlights the critical advantage of explicitly modeling and utilizing latent post-serving dynamics, provided the learning algorithm is robust enough to handle the associated corruptions and delays.

Further experimental results, including sensitivity analyses regarding context dimensionality, arm set size, and error budgets, alongside evaluations on real-world datasets, are detailed in Section E of the supplementary material.

7. Conclusion and Discussion

In this work, we introduced RCDP-UCB, a unified framework for linear contextual dueling bandits designed to robustly handle latent post-serving contexts, adversarial corruptions, and unknown feedback delays. By anchoring our analysis to the full information design matrix \tilde{V}_{t-1} , we developed an adaptive weighting mechanism operating on a unified error budget $\mathcal{C} + \mathcal{D}$. This design enables the algorithm to determine importance weights *a priori*, effectively decoupling parameter estimation from the specific realization of delay sequences. Theoretically, RCDP-UCB achieves sublinear regret while remaining agnostic to the underlying delay regime; our bounds match information-theoretic lower bounds up to logarithmic factors in the stochastic setting and remain near-optimal within a \sqrt{d} factor in the adversarial delay regime.

Limitations. A critical direction for future research is extending this framework to handle delayed post-serving contexts. Additionally, closing the $\mathcal{O}(\sqrt{d})$ gap in the adversarial delay lower bound remains an open problem. Additionally, establishing a tight information-theoretic lower bound that explicitly accounts for the learnability of post-serving mappings remains an open problem.

Impact Statement

This paper presents a robust algorithmic framework for interactive decision-making, with significant implications for enhancing the reliability of systems reliant on human feedback, such as recommendation engines and Reinforcement Learning from Human Feedback (RLHF). By effectively mitigating the risks associated with adversarial data poisoning and feedback delays, our work contributes to the development of safer AI systems that are resilient to manipulation. Furthermore, the integration of latent post-serving contexts promotes a more accurate alignment with genuine user intent, moving beyond superficial engagement metrics. While our primary focus is on robustness, we encourage practitioners to carefully calibrate these mechanisms to ensure that legitimate minority feedback is not inadvertently filtered out as adversarial noise.

References

- Abbasi-Yadkori, Y., Pál, D., and Szepesvári, C. Improved algorithms for linear stochastic bandits. *Advances in neural information processing systems*, 24, 2011.
- Achiam, J., Adler, S., Agarwal, S., Ahmad, L., Akkaya, I., Aleman, F. L., Almeida, D., Altenschmidt, J., Altman, S., Anadkat, S., et al. Gpt-4 technical report. *arXiv preprint arXiv:2303.08774*, 2023.
- Agarwal, A., Agarwal, S., and Patil, P. Stochastic dueling bandits with adversarial corruption. In *Proceedings of Algorithmic Learning Theory (ALT)*, pp. 217–248, 2021.
- Bengs, V., Saha, A., and Hüllermeier, E. Stochastic contextual dueling bandits under linear stochastic transitivity models. In *International Conference on Machine Learning*, pp. 1764–1786. PMLR, 2022.
- Di, Q., Jin, T., Wu, Y., Zhao, H., Farnoud, F., and Gu, Q. Variance-aware regret bounds for stochastic contextual dueling bandits. In *The Twelfth International Conference on Learning Representations*, 2023.
- Di, Q., He, J., and Gu, Q. Nearly optimal algorithms for contextual dueling bandits from adversarial feedback. *arXiv preprint arXiv:2404.10776*, 2024.
- Dudík, M., Hofmann, K., Schapire, R. E., Slivkins, A., and Zoghi, M. Contextual dueling bandits. In *Conference on Learning Theory*, pp. 563–587. PMLR, 2015.
- Filippi, S., Cappe, O., Garivier, A., and Szepesvári, C. Parametric bandits: The generalized linear case. *Advances in neural information processing systems*, 23, 2010.
- Guo, D., Yang, D., Zhang, H., Song, J., Zhang, R., Xu, R., Zhu, Q., Ma, S., Wang, P., Bi, X., et al. Deepseek-r1: Incentivizing reasoning capability in llms via reinforcement learning. *arXiv preprint arXiv:2501.12948*, 2025.
- Gupta, A., Koren, T., and Talwar, K. Better algorithms for stochastic bandits with adversarial corruptions. In *Conference on Learning Theory*, pp. 1562–1578. PMLR, 2019.
- He, J., Zhou, D., Zhang, T., and Gu, Q. Nearly optimal algorithms for linear contextual bandits with adversarial corruptions. In *Advances in Neural Information Processing Systems (NeurIPS)*, 2022.
- Howson, B., Pike-Burke, C., and Filippi, S. Delayed feedback in generalised linear bandits revisited. In *International Conference on Artificial Intelligence and Statistics*, pp. 6095–6119. PMLR, 2023.
- Hunter, D. R. Mm algorithms for generalized bradley-terry models. *The annals of statistics*, 32(1):384–406, 2004.
- Ito, S., Hatano, D., Sumita, H., Takemura, K., Fukunaga, T., Kakimura, N., and Kawarabayashi, K.-I. Delay and cooperation in nonstochastic linear bandits. *Advances in Neural Information Processing Systems*, 33:4872–4883, 2020.
- Kingma, D. P. Adam: A method for stochastic optimization. *arXiv preprint arXiv:1412.6980*, 2014.
- Lancewicki, T. et al. A unified analysis of nonstochastic delayed feedback for combinatorial semi-bandits, linear bandits, and mdps. In *Conference on Learning Theory (COLT)*, 2023.
- Lattimore, T. and Szepesvári, C. *Bandit algorithms*. Cambridge University Press, 2020.
- Li, X., Zhao, H., and Gu, Q. Feel-good thompson sampling for contextual dueling bandits. *arXiv preprint arXiv:2404.06013*, 2024.
- Liu, H., Tajdini, A., Wagenmaker, A., and Wei, C.-Y. Corruption-robust linear bandits: Minimax optimality and gap-dependent misspecification. *Advances in Neural Information Processing Systems*, 37:24277–24325, 2024.
- Luce, R. D. *Individual choice behavior: A theoretical analysis*. Courier Corporation, 2005.
- Ouyang, L., Wu, J., Jiang, X., Almeida, D., Wainwright, C., Mishkin, P., Zhang, C., Agarwal, S., Slama, K., Ray, A., et al. Training language models to follow instructions with human feedback. *Advances in neural information processing systems*, 35:27730–27744, 2022.
- Park, H. and Faradonbeh, M. K. S. Analysis of thompson sampling for partially observable contextual multi-armed bandits. *IEEE Control Systems Letters*, 6:2150–2155, 2021.

- Pike-Burke, C., Agrawal, S., Szepesvari, C., and Grunewalder, S. Bandits with delayed, aggregated anonymous feedback. In *International Conference on Machine Learning*, pp. 4105–4113. PMLR, 2018.
- Qi, Y., Wu, Q., Wang, H., Tang, J., and Sun, M. Bandit learning with implicit feedback. *Advances in Neural Information Processing Systems*, 31, 2018.
- Rafailov, R., Sharma, A., Mitchell, E., Manning, C. D., Ermon, S., and Finn, C. Direct preference optimization: Your language model is secretly a reward model. *Advances in neural information processing systems*, 36: 53728–53741, 2023.
- Saha, A. Optimal algorithms for stochastic contextual preference bandits. *Advances in Neural Information Processing Systems*, 34:30050–30062, 2021.
- Srinivas, N., Krause, A., Kakade, S. M., and Seeger, M. W. Information-theoretic regret bounds for gaussian process optimization in the bandit setting. *IEEE transactions on information theory*, 58(5):3250–3265, 2012.
- Tsybakov, A. B. Nonparametric estimators. In *Introduction to Nonparametric Estimation*, pp. 1–76. Springer, 2008.
- Vernade, C., Carpentier, A., Lattimore, T., Zappella, G., Ermis, B., and Brueckner, M. Linear bandits with stochastic delayed feedback. In *International Conference on Machine Learning (ICML)*, 2020.
- Wang, C., Ye, Z., Feng, Z., Badanidiyuru Varadaraja, A., and Xu, H. Follow-ups also matter: Improving contextual bandits via post-serving contexts. *Advances in Neural Information Processing Systems*, 36, 2024.
- Wang, H., Wu, Q., and Wang, H. Learning hidden features for contextual bandits. In *Proceedings of the 25th ACM international on conference on information and knowledge management*, pp. 1633–1642, 2016.
- Yang, J. and Ren, S. Robust bandit learning with imperfect context. In *Proceedings of the AAAI Conference on Artificial Intelligence*, volume 35, pp. 10594–10602, 2021.
- Yang, S., Wang, H., Zhang, C., and Gao, Y. Contextual bandits with hidden features to online recommendation via sparse interactions. *IEEE intelligent systems*, 35(5): 62–72, 2020.
- Ye, C., Xiong, W., Gu, Q., and Zhang, T. Corruption-robust algorithms with uncertainty weighting for nonlinear contextual bandits and markov decision processes. In *International Conference on Machine Learning*, pp. 39834–39863. PMLR, 2023.
- Yu, Q., Baek, E., Li, X., and Sun, Q. Corruption-robust variance-aware algorithms for generalized linear bandits under heavy-tailed rewards. In Chiappa, S. and Magliacane, S. (eds.), *Proceedings of the Forty-first Conference on Uncertainty in Artificial Intelligence*, volume 286 of *Proceedings of Machine Learning Research*, pp. 4826–4843. PMLR, 21–25 Jul 2025. URL <https://proceedings.mlr.press/v286/yu25b.html>.
- Yue, Y., Broder, J., Kleinberg, R., and Joachims, T. The k-armed dueling bandits problem. *Journal of Computer and System Sciences*, 78(5):1538–1556, 2012.
- Zhou, Z., Xu, R., and Blanchet, J. Learning in generalized linear contextual bandits with stochastic delays. *Advances in Neural Information Processing Systems*, 32, 2019.
- Zhu, R. and Kveton, B. Robust contextual linear bandits. *arXiv preprint arXiv:2210.14483*, 2022.

Supplementary Material:

Robust Linear Dueling Bandits with Post-serving Context under Unknown Delays and Adversarial Corruptions

In Section A, we derive the concentration bound for parameter estimation error under the dual challenges of adversarial corruptions and delayed feedback. We then provide the complete proof for the regret upper bound of Theorem 5.2 in Section B, followed by the proof of the lower bound (Theorem 5.3) in Section C. Finally, in Section D, we provide implementation details for the experimental results in Section 6, ablation studies varying the dimension of arms and contexts, the corruption budget \mathcal{C} , and delay complexity \mathcal{D} , as well as additional results regarding hyperparameter sensitivity and baseline comparisons.

A. Proof of Lemma 5.1

The following lemma is a weighted generalization of the self-normalized bound for vector-valued martingales (Abbasi-Yadkori et al., 2011).

Lemma A.1 (Weighted Self-Normalized Bound). *Let $\{\mathcal{F}_t\}_{t=0}^\infty$ be a filtration. Let $\{\varepsilon_s\}_{s \geq 1}$ be a real-valued process such that ε_s is \mathcal{F}_s -measurable and conditionally R -sub-Gaussian. Let $\{\Delta z_s\}_{s \geq 1}$ be an \mathbb{R}^d -valued process where Δz_s is \mathcal{F}_{s-1} -measurable and $\|\Delta z_s\|_2 \leq L$. For any sequence of predictable weights $\omega_s \in (0, 1]$ and scaling factor $\kappa > 0$, define $\mathcal{S}_t = \sum_{s=1}^t \omega_s \varepsilon_s \Delta z_s$ and $\tilde{V}_t = \lambda I + \kappa \sum_{s=1}^t \omega_s \Delta z_s \Delta z_s^\top$. Then, for any $\delta > 0$, with probability at least $1 - \delta$, the following inequality holds for all $t \geq 1$:*

$$\|\mathcal{S}_t\|_{\tilde{V}_t^{-1}} \leq \frac{R\sqrt{\bar{\omega}}}{\sqrt{\kappa}} \sqrt{2 \log \left(\frac{\det(\tilde{V}_t)^{1/2}}{\delta \det(\lambda I)^{1/2}} \right)},$$

where $\bar{\omega} = \max_{s \leq t} \omega_s$. By the determinant-trace inequality, it holds that:

$$\|\mathcal{S}_t\|_{\tilde{V}_t^{-1}} \leq \frac{R\sqrt{\bar{\omega}}}{\sqrt{\kappa}} \sqrt{d \log \left(1 + \frac{\kappa t L^2 \bar{\omega}}{d \lambda} \right) + 2 \log \left(\frac{1}{\delta} \right)}.$$

Proof. Define the transformed covariates $X_s := \sqrt{\kappa \omega_s} \Delta z_s$ and the scaled noise terms $\epsilon_s := \sqrt{\omega_s / \kappa} \varepsilon_s$. Under the assumption that ω_s is \mathcal{F}_{s-1} -measurable and $\omega_s \in (0, 1]$, ϵ_s is conditionally R' -sub-Gaussian with $R' = R\sqrt{\omega_s / \kappa} \leq R\sqrt{\bar{\omega}} / \kappa$. The martingale sum and the design matrix then take the standard forms:

$$\mathcal{S}_t = \sum_{s=1}^t \epsilon_s X_s, \quad \text{and} \quad \tilde{V}_t = \lambda I + \sum_{s=1}^t X_s X_s^\top.$$

Directly applying Theorem 1 from Abbasi-Yadkori et al. (2011) to the pair (X_s, ϵ_s) with the uniform sub-Gaussian proxy $R\sqrt{\bar{\omega}} / \kappa$ yields the self-normalized bound. The final result follows by substituting the determinant-trace inequality $\log(\det(\tilde{V}_t) / \det(\lambda I)) \leq d \log(1 + \frac{\kappa t L^2 \bar{\omega}}{d \lambda})$. \square

Lemma A.2 (Bound on Invisible Feedbacks). *Let $D_t := \sum_{s=1}^{t-1} \mathbb{1}_{s+\tau_s > t}$ denote the number of invisible feedbacks at time t , where τ_s is the delay associated with the feedback from round s . Let Λ denote the cumulative delay budget, and let μ_τ denote the mean of sub-Gaussian delays. Then, for any $t \in [T]$, with probability at least $1 - \delta$:*

$$D_t = \tilde{\mathcal{O}}(\mathcal{D}), \quad \text{where} \quad \mathcal{D} := \max(\sqrt{\Lambda}, \max(\mu_\tau, 1)). \quad (\text{A.1})$$

Proof. We consider the two delay models separately.

Stochastic Delays. By Lemma 4 in (Howson et al., 2023), for sub-Gaussian delays:

$$D_t = \tilde{\mathcal{O}}(\mu_\tau + \sqrt{\mu_\tau \log(1/\delta)} + 1) = \tilde{\mathcal{O}}(\max(\mu_\tau, 1)). \quad (\text{A.2})$$

Adversarial Delays. Let $\mathcal{S}_t := \{s < t : s + \tau_s > t\}$ denote the set of indices with pending feedback at time t , so that $D_t = |\mathcal{S}_t|$. For each $s \in \mathcal{S}_t$, the feedback is invisible only if the delay satisfies $\tau_s > t - s$. Since delays are integer-valued, this implies $\tau_s \geq t - s + 1$.

The total delay budget provides a lower bound:

$$\Lambda = \sum_{s=1}^T \tau_s \geq \sum_{s \in \mathcal{S}_t} \tau_s \geq \sum_{s \in \mathcal{S}_t} (t - s + 1).$$

To minimize this sum for a fixed cardinality D_t , the adversary acts greedily by choosing the indices closest to t , namely $s \in \{t - 1, t - 2, \dots, t - D_t\}$. Substituting $k = t - s$, the sum becomes:

$$\Lambda \geq \sum_{k=1}^{D_t} (k + 1) = \frac{D_t(D_t + 1)}{2} + D_t = \frac{D_t^2 + 3D_t}{2} \geq \frac{D_t^2}{2}.$$

Inverting this quadratic inequality yields the bound on the number of invisible feedbacks:

$$D_t \leq \sqrt{2\Lambda}. \quad (\text{A.3})$$

Combining Eq. (A.2) and Eq. (A.3) yields Eq. (A.1). \square

We define by introducing auxiliary quantities that will be instrumental in our analysis:

$$\begin{aligned} \eta_t &:= l_t - g(\Delta z_t^\top \Theta_*), \\ \zeta_t &:= \gamma_t - g(\Delta z_t^\top \Theta_*), \end{aligned}$$

where l_t denotes the unobserved true feedback, γ_t represents the corrupted observation, $g(\cdot)$ is the link function, and Θ_* is the true underlying parameter. Additionally, we define the auxiliary function $G_t : \mathbb{R}^d \rightarrow \mathbb{R}^d$ as:

$$G_t(\Theta) := \lambda \Theta + \sum_{s=1}^{t-1} \omega_s (g(\Theta^\top \Delta z_s) - g(\Theta_*^\top \Delta z_s)) \Delta z_s,$$

where ω_s denotes the adaptive weight assigned to the s -th observation as Equation (4).

Step 1: Error Decomposition via Local Strong Convexity

By the Mean Value Theorem, for any $\Theta_1, \Theta_2 \in \mathbb{R}^d$, there exists $\bar{\Theta}$ on the line segment connecting them such that:

$$G_t(\Theta_1) - G_t(\Theta_2) = \nabla G_t(\bar{\Theta})(\Theta_1 - \Theta_2) = H_t(\bar{\Theta})(\Theta_1 - \Theta_2),$$

where the Hessian matrix $H_t(\bar{\Theta})$ is given by:

$$H_t(\bar{\Theta}) := \lambda I + \sum_{s=1}^{t-1} \omega_s \dot{g}(\bar{\Theta}^\top \Delta z_s) \Delta z_s \Delta z_s^\top.$$

with $\lambda > 0$. Since $\dot{g}(\cdot) \geq \kappa > 0$ by Assumption 4.1, we have the matrix domination $H_t(\bar{\Theta}) \succeq \tilde{V}_{t-1}$, where:

$$\tilde{V}_{t-1} := \lambda I + \kappa \sum_{s=1}^{t-1} \omega_s \Delta z_s \Delta z_s^\top.$$

as in Equation (1). Utilizing the identity $\|Ax\|_{A^{-1}} = \|x\|_A$ for any positive definite matrix A , we obtain the following monotonicity property:

$$\|G_t(\Theta_1) - G_t(\Theta_2)\|_{\tilde{V}_{t-1}^{-1}} \geq \|\Theta_1 - \Theta_2\|_{\tilde{V}_{t-1}}. \quad (\text{A.4})$$

Note that

$$G_t(\Theta_*) = \lambda\Theta_*$$

by the definition of G_t . Let Θ_t be the estimator satisfying Eq. (3). By the optimality condition, we have:

$$\lambda\Theta_t + \sum_{s=1}^{t-1} \omega_s \mathbb{I}_{s+\tau_s \leq t} (g(\Theta_t^\top \Delta z_s) - o_s) \Delta z_s = 0, \quad (\text{A.5})$$

where $\mathbb{I}_{s+\tau_s \leq t}$ is the indicator function for whether the feedback from round s has arrived by time t , and o_s denotes the observed (potentially corrupted) feedback.

Using Eq. (A.5), we decompose $G_t(\Theta_t)$ into three components:

$$\begin{aligned} G_t(\Theta_t) &= \lambda\Theta_t + \sum_{s=1}^{t-1} \omega_s (g(\Theta_t^\top \Delta z_s) - g(\Theta_*^\top \Delta z_s)) \Delta z_s \\ &= \underbrace{\sum_{s=1}^{t-1} \mathbb{I}_{s+\tau_s \leq t} \omega_s (o_s - g(\Theta_*^\top \Delta z_s)) \Delta z_s}_{S_{t,1}} \\ &\quad + \underbrace{\sum_{s=1}^{t-1} (1 - \mathbb{I}_{s+\tau_s \leq t}) \omega_s (g(\Theta_t^\top \Delta z_s) - o_s) \Delta z_s}_{S_{t,2}} \\ &\quad - \underbrace{\sum_{s=1}^{t-1} (1 - \mathbb{I}_{s+\tau_s \leq t}) \omega_s (g(\Theta_*^\top \Delta z_s) - o_s) \Delta z_s}_{S_{t,3}}. \end{aligned} \quad (\text{A.6})$$

In Equation (A.6), the term $S_{t,1}$ captures the contribution from observed feedback, while $S_{t,2}$ and $S_{t,3}$ account for the missing information due to delayed feedback.

Step 2: Calculation of $S_{t,1}$

Let $C_s \in \{0, 1\}$ denote the corruption indicator at round s , where $C_s = 1$ indicates that the feedback has been corrupted (unknownst to the learner). We decompose $S_{t,1}$ as:

$$\begin{aligned} S_{t,1} &= \sum_{\substack{s=1 \\ C_s=0}}^{t-1} \mathbb{I}_{s+\tau_s \leq t} \omega_s \eta_s \Delta z_s + \sum_{\substack{s=1 \\ C_s=1}}^{t-1} \mathbb{I}_{s+\tau_s \leq t} \omega_s (\gamma_s - \eta_s + \eta_s) \Delta z_s \\ &= \sum_{s=1}^{t-1} \mathbb{I}_{s+\tau_s \leq t} \omega_s \eta_s \Delta z_s + \sum_{\substack{s=1 \\ C_s=1}}^{t-1} \mathbb{I}_{s+\tau_s \leq t} \omega_s (\gamma_s - \eta_s) \Delta z_s \\ &=: S_{t,1,1} + S_{t,1,2}. \end{aligned}$$

The term $S_{t,1,1}$ corresponds to the stochastic noise contribution, while $S_{t,1,2}$ captures the adversarial corruption effect.

A key technical challenge arises because $S_{t,1,1}$ is not a martingale when delays are chosen adaptively by an adversary—the terms $\mathbb{E}[\eta_s]$ and $\mathbb{I}_{s+\tau_s \leq t}$ may exhibit dependence. To address this, we perform a further decomposition:

$$S_{t,1,1} = \underbrace{\sum_{s=1}^{t-1} \omega_s \eta_s \Delta z_s}_{S_{t,1,1,1}} - \underbrace{\sum_{s=1}^{t-1} \mathbb{I}_{s+\tau_s > t} \omega_s \eta_s \Delta z_s}_{S_{t,1,1,2}}.$$

The term $S_{t,1,1,1}$ is now a proper martingale with respect to the natural filtration, while $S_{t,1,1,2}$ captures the contribution from observations whose feedback has not yet arrived.

Applying Lemma A.1 to $S_{t,1,1,1}$ with $R = 1/2$ (corresponding to the Gaussian prior $\mathcal{N}(0, \lambda^{-1}I)$ settings) and $\bar{\omega} = 1$, we obtain that with probability at least $1 - \delta$:

$$\|S_{t,1,1,1}\|_{\tilde{V}_t^{-1}} \leq C \sqrt{d \log \left(\frac{1 + tL^2/(d\lambda)}{\delta} \right)},$$

for some constant $C = C(\kappa) > 0$.

For the delayed feedback term $S_{t,1,1,2}$, note that η_s may not be observed to the learner yet. However, we already know that $|\eta_s| \leq 1$. Accordingly, we have:

$$\|S_{t,1,1,2}\|_{\tilde{V}_t^{-1}} \leq \sum_{s=1}^{t-1} \mathbb{I}_{s+\tau_s > t} \omega_s \|\Delta z_s\|_{\tilde{V}_t^{-1}} \leq \alpha D_t,$$

due to $\omega_s = \min(1, \alpha/\|\Delta z_s\|_{\tilde{V}_{s-1}^{-1}})$, where $D_t := \sum_{s=1}^{t-1} \mathbb{I}_{s+\tau_s > t}$ denotes the number of invisible (pending) feedbacks at time t . Thus,

$$\|S_{t,1,1}\|_{\tilde{V}_t^{-1}} \leq C \sqrt{d \log \left(\frac{1 + tL^2/(d\lambda)}{\delta} \right)} + \alpha D_t. \quad (\text{A.7})$$

For the corruption term $S_{t,1,2}$, the design of adaptive weights $\omega_s = \min(1, \alpha/\|\Delta z_s\|_{\tilde{V}_{s-1}^{-1}})$ yields:

$$\|S_{t,1,2}\|_{\tilde{V}_t^{-1}} \leq \sum_{\substack{s=1 \\ \mathcal{C}_s=1}}^{t-1} \omega_s \|\Delta z_s\|_{\tilde{V}_t^{-1}} \leq \mathcal{C} \alpha, \quad (\text{A.8})$$

where \mathcal{C} denotes the total corruption budget. As a result, combining Equations (A.7) and (A.8), we obtain

$$\|S_{t,1}\|_{\tilde{V}_t^{-1}} \leq C \sqrt{d \log \left(\frac{1 + tL^2/(d\lambda)}{\delta} \right)} + \alpha \mathcal{C} + \alpha D_t. \quad (\text{A.9})$$

Step 2: Calculation of $S_{t,2}$ and $S_{t,3}$

For the terms $S_{t,2}$ and $S_{t,3}$ arising from pending feedback, using $\omega_s > 0$ and $|g(\Theta_*^\top \Delta z_s) - o_s| \leq 1$, we obtain:

$$\begin{aligned} \|S_{t,2}\|_{\tilde{V}_t^{-1}} + \|S_{t,3}\|_{\tilde{V}_t^{-1}} &\leq 2 \sum_{s=1}^{t-1} \mathbb{I}_{s+\tau_s > t} \omega_s \|\Delta z_s\|_{\tilde{V}_t^{-1}} \\ &\leq 2\alpha \sum_{s=1}^{t-1} \mathbb{I}_{s+\tau_s > t} = 2\alpha D_t. \end{aligned} \quad (\text{A.10})$$

Step 3: Final Error Bound

Utilizing Lemma A.2, we can obtain

$$\alpha D_t = \alpha \tilde{\mathcal{O}}(\mathcal{D}),$$

where $\mathcal{D} = \max(\Lambda^{1/2}, \mu_\tau)$. Accordingly, setting the robustness parameter α as:

$$\alpha = \frac{\sqrt{d}}{\mathcal{C} + \mathcal{D}},$$

and combining the bounds from Eqs. (A.4), (A.9) and (A.10), we obtain:

$$\|\Theta_t - \Theta_*\|_{\tilde{V}_t^{-1}} = \tilde{\mathcal{O}}(\sqrt{d}).$$

due to Lemma A.2. Finally, since $\widetilde{W}_{t-1} \preceq \widetilde{V}_{t-1}$, we have:

$$\|\Theta_t - \Theta_*\|_{\widetilde{W}_{t-1}} \leq \|\Theta_t - \Theta_*\|_{\widetilde{V}_{t-1}} \leq \beta_t,$$

where the confidence radius is given by:

$$\beta_t := \frac{1}{2} \sqrt{d \log \left(\frac{1 + tL^2/(d\lambda)}{\delta} \right)} + \sqrt{d} \frac{C}{C + \mathcal{D}} + \sqrt{\lambda} \|\Theta_*\| + \sqrt{d} \frac{3\mathcal{D}}{C + \mathcal{D}}.$$

This completes the proof. □

B. Proof of Theorem 5.2

We first state the generalized elliptic potential lemma.

Lemma B.1 (Generalized Elliptical Potential Lemma (Wang et al., 2024)). *Suppose*

1. $X_0 \in \mathbb{R}^{d \times d}$ is any positive definite matrix;
2. $x_1, \dots, x_T \in \mathbb{R}^d$ is a sequence of vectors with bounded ℓ_2 norm $\max_t \|x_t\| \leq L_x$;
3. $\epsilon_1, \dots, \epsilon_T \in \mathbb{R}^d$ is a sequence of independent (not necessarily identical) bounded zero-mean noises satisfying $\max_t \|\epsilon_t\| \leq L_\epsilon$ and $\mathbb{E}[\epsilon_t \epsilon_t^\top] \succeq \sigma_\epsilon^2 I$ for any t ; and
4. \widetilde{X}_t is defined as follows:

$$\widetilde{X}_t = X_0 + \sum_{s=1}^t (x_s + \epsilon_s)(x_s + \epsilon_s)^\top \in \mathbb{R}^{d \times d}.$$

Then, for any $p \in [0, 1]$, the following inequality holds with probability at least $1 - \delta$,

$$\sum_{t=1}^T \left(1 \wedge \|x_t\|_{\widetilde{X}_{t-1}}^2 \right)^p \leq 2^p T^{1-p} \log^p \left(\frac{\det X_T}{\det X_0} \right) + \frac{8L_\epsilon^2 (L_\epsilon + L_x)^2}{\sigma_\epsilon^4} \log \left(\frac{32dL_\epsilon^2 (L_\epsilon + L_x)^2}{\delta \sigma_\epsilon^4} \right)$$

where $a \wedge b = \min\{a, b\}$.

For clarity, we define the key quantities used throughout the proof. For each round $t \in [T]$ and arm $k \in [K]$, we define three variants of the joint feature vector:

$$\begin{aligned} \widehat{z}_{t,k} &:= (x_{t,k}, \widehat{\phi}_t(x_{t,k})), \\ z_{t,k}^* &:= (x_{t,k}, \phi_*(x_{t,k})), \\ z_{t,k} &:= (x_{t,k}, y_{t,k}), \end{aligned}$$

where $\widehat{\phi}_t$ denotes the learner's estimate of the true post-serving function ϕ_* at round t , and $y_{t,k}$ is the observed post-serving context. Additionally, we use the shorthand notation $\Delta z_{t,k,k'} := z_{t,k} - z_{t,k'}$ for differences between feature vectors, and analogously for $\Delta \widehat{z}_{t,k,k'}$ and $\Delta z_{t,k,k'}^*$.

Step 1: Analysis of Instantaneous Regret

The proof proceeds by decomposing the instantaneous regret into three interpretable components and bounding each term separately. Let k_t^* denote the optimal arm at round t , and let a_t and b_t denote the arms selected by our algorithm according to Equation (5)–Equation (6). The instantaneous regret r_t satisfies:

$$2r_t = \langle \Theta_*, \Delta z_{t,k_t^*,a_t}^* + \Delta z_{t,k_t^*,b_t}^* \rangle.$$

We decompose this quantity into three components by adding and subtracting appropriate terms:

$$\begin{aligned}
 2r_t &= \underbrace{\langle \Theta_t, \Delta \widehat{z}_{t,k_t^*,a_t} + \Delta \widehat{z}_{t,k_t^*,b_t} \rangle}_{\mathcal{B}_{t,1}: \text{Confidence Interval Term}} \\
 &+ \underbrace{\langle \Theta_*, (\Delta z_{t,k_t^*,a_t}^* - \Delta \widehat{z}_{t,k_t^*,a_t}) + (\Delta z_{t,k_t^*,b_t}^* - \Delta \widehat{z}_{t,k_t^*,b_t}) \rangle}_{\mathcal{B}_{t,2}: \text{Approximation Error Term}} \\
 &+ \underbrace{\langle \Theta_* - \Theta_t, \Delta \widehat{z}_{t,k_t^*,a_t} + \Delta \widehat{z}_{t,k_t^*,b_t} \rangle}_{\mathcal{B}_{t,3}: \text{Estimation Error Term}}.
 \end{aligned}$$

The first term $\mathcal{B}_{t,1}$ captures the suboptimality arising from the algorithm's arm selection rule under the current parameter estimate. The second term $\mathcal{B}_{t,2}$ quantifies the regret induced by the discrepancy between the true post-serving function and its approximation. The third term $\mathcal{B}_{t,3}$ reflects the estimation error in the parameter.

Step 1: Bounding the Confidence Interval Term $\mathcal{B}_{t,1}$

To estimate $\mathcal{B}_{t,1}$, we consider the arm selection strategy specified in Equation (5)–Equation (6). The selected arms a_t and b_t satisfy:

$$\langle \Theta_t, \widehat{z}_{t,k_t^*} \rangle \leq \langle \Theta_t, \widehat{z}_{t,a_t} \rangle, \quad (\text{B.11})$$

$$\langle \Theta_t, \widehat{z}_{t,k} \rangle + c_t \|\Delta \widehat{z}_{t,k,a_t}\|_{\widetilde{V}_{t-1}^{-1}} \leq \langle \Theta_t, \widehat{z}_{t,b_t} \rangle + c_t \|\Delta \widehat{z}_{t,b_t,a_t}\|_{\widetilde{V}_{t-1}^{-1}}, \quad (\text{B.12})$$

for all $k \in \mathcal{K}_t$. Using the identity

$$\Delta \widehat{z}_{t,k_t^*,a_t} + \Delta \widehat{z}_{t,k_t^*,b_t} = 2\Delta \widehat{z}_{t,k_t^*,a_t} + \Delta \widehat{z}_{t,a_t,b_t} \quad (\text{B.13})$$

and applying (B.11)–(B.12), we obtain:

$$\begin{aligned}
 \mathcal{B}_{t,1} &= \langle \Theta_t, 2\Delta \widehat{z}_{t,k_t^*,a_t} + \Delta \widehat{z}_{t,a_t,b_t} \rangle \\
 &\leq \langle \Theta_t, \Delta \widehat{z}_{t,k_t^*,a_t} \rangle + \langle \Theta_t, \Delta \widehat{z}_{t,a_t,b_t} \rangle \\
 &\leq c_t (\|\Delta \widehat{z}_{t,b_t,a_t}\|_{\widetilde{V}_{t-1}^{-1}} - \|\Delta \widehat{z}_{t,k_t^*,a_t}\|_{\widetilde{V}_{t-1}^{-1}}).
 \end{aligned} \quad (\text{B.14})$$

The term $\mathcal{B}_{t,2}$ captures the regret induced by the discrepancy between the true post-serving contexts $z_{t,k}^*$ and the learner's approximations $\widehat{z}_{t,k}$. Observe that by construction:

$$z_{t,k}^* - \widehat{z}_{t,k} = (0, \phi_*(x_{t,k}) - \widehat{\phi}_t(x_{t,k})).$$

Applying the Cauchy–Schwarz inequality and Assumption 4.2, we have for any arm k :

$$|\langle \Theta_*, z_{t,k}^* - \widehat{z}_{t,k} \rangle| \leq \|\Theta_*\|_2 \cdot \|\phi_*(x_{t,k}) - \widehat{\phi}_t(x_{t,k})\|_2 \leq M \|\phi_*(x_{t,k}) - \widehat{\phi}_t(x_{t,k})\|_2.$$

By Assumption 4.3 (General Learnability), with probability at least $1 - \delta$, the approximation error satisfies:

$$\|\phi_*(x_{t,k}) - \widehat{\phi}_t(x_{t,k})\|_2 \leq C_0 \sqrt{d_x} t^{-\nu} \log(t/\delta),$$

for some universal constant $C_0 > 0$. Combining these bounds and applying the triangle inequality over both arm pairs, we obtain:

$$\mathcal{B}_{t,2} \leq 4MC_0 \sqrt{d_x} t^{-\nu} \log(t/\delta). \quad (\text{B.15})$$

For the estimation error term $\mathcal{B}_{t,3}$, we apply the confidence ellipsoid property. By Lemma 5.1, the parameter estimate Θ_t satisfies:

$$\|\Theta_* - \Theta_t\|_{\widetilde{V}_{t-1}} \leq \beta_t,$$

where β_t is the confidence radius. Applying this bound together with the Cauchy–Schwarz inequality and Equation (B.13) yields:

$$\begin{aligned} \mathcal{B}_{3,t} &= \langle \Theta_* - \Theta_t, \Delta \widehat{z}_{t,k_t^*,a_t} + \Delta \widehat{z}_{t,k_t^*,b_t} \rangle \\ &\leq \|\Theta_* - \Theta_t\|_{\widetilde{V}_{t-1}^{-1}} \left(2\|\Delta \widehat{z}_{t,k_t^*,a_t}\|_{\widetilde{V}_{t-1}^{-1}} + \|\Delta \widehat{z}_{t,a_t,b_t}\|_{\widetilde{V}_{t-1}^{-1}} \right) \\ &\leq 2\beta_t \|\Delta \widehat{z}_{t,k_t^*,a_t}\|_{\widetilde{V}_{t-1}^{-1}} + \beta_t \|\Delta \widehat{z}_{t,a_t,b_t}\|_{\widetilde{V}_{t-1}^{-1}}. \end{aligned} \quad (\text{B.16})$$

Setting $c_t = 2\beta_t$ and combining (B.14), (B.15), and (B.16), the instantaneous regret satisfies:

$$2r_t \leq 3\beta_t \|\Delta \widehat{z}_{t,a_t,b_t}\|_{\widetilde{V}_{t-1}^{-1}} + 4C_0 M \sqrt{d_x} t^{-\nu} \log(t/\delta).$$

Step 2: Cumulative Regret Analysis

Summing over all rounds $t \in [T]$, the cumulative regret $R_T = \sum_{t=1}^T r_t$ satisfies:

$$2R_T \leq 3\beta_T \sum_{t=1}^T \|\Delta \widehat{z}_{t,a_t,b_t}\|_{\widetilde{V}_{t-1}^{-1}} + 4C_0 M \sqrt{d_x} \log(T/\delta) \sum_{t=1}^T t^{-\nu}. \quad (\text{B.17})$$

We further decompose the first sum by relating the approximated features to the true features:

$$\sum_{t=1}^T \|\Delta \widehat{z}_{t,a_t,b_t}\|_{\widetilde{V}_{t-1}^{-1}} \leq \sum_{t=1}^T \|\Delta z_{t,a_t,b_t}^*\|_{\widetilde{V}_{t-1}^{-1}} + \sum_{t=1}^T \|\Delta z_{t,a_t,b_t}^* - \Delta \widehat{z}_{t,a_t,b_t}\|_{\widetilde{V}_{t-1}^{-1}}.$$

By the eigenvalue bound $\|\cdot\|_{\widetilde{V}_{t-1}^{-1}} \leq \lambda^{-1/2} \|\cdot\|_2$ and Assumption 4.3:

$$\begin{aligned} \sum_{t=1}^T \|\Delta z_{t,a_t,b_t}^* - \Delta \widehat{z}_{t,a_t,b_t}\|_{\widetilde{V}_{t-1}^{-1}} &\leq \frac{1}{\sqrt{\lambda}} \sum_{t=1}^T \|\Delta z_{t,a_t,b_t}^* - \Delta \widehat{z}_{t,a_t,b_t}\|_2 \\ &\leq \frac{2}{\sqrt{\lambda}} \sum_{t=1}^T (\|\widehat{\phi}_t(x_{t,a_t}) - \phi_*(x_{t,a_t})\|_2 + \|\widehat{\phi}_t(x_{t,b_t}) - \phi_*(x_{t,b_t})\|_2) \\ &\leq \frac{4C_0 \sqrt{d_x}}{\sqrt{\lambda}} \log(T/\delta) \sum_{t=1}^T t^{-\nu}. \end{aligned}$$

For $\nu \in (0, 1)$, we employ the integral comparison:

$$\sum_{t=1}^T t^{-\nu} \leq \int_0^T x^{-\nu} dx = \frac{T^{1-\nu}}{1-\nu}.$$

Thus,

$$\sum_{t=1}^T \|\Delta z_{t,a_t,b_t}^* - \Delta \widehat{z}_{t,a_t,b_t}\|_{\widetilde{V}_{t-1}^{-1}} \leq \frac{4C_0 \sqrt{d_x}}{\sqrt{\lambda}} \log(T/\delta) \frac{T^{1-\nu}}{1-\nu}.$$

We partition the sum based on the weighting scheme:

$$\begin{aligned}
 \sum_{t=1}^T \|\Delta z_{t,a_t,b_t}^* \|_{\tilde{V}_{t-1}^{-1}} &= \sum_{t:\omega_t=1} \|\Delta z_{t,a_t,b_t}^* \|_{\tilde{V}_{t-1}^{-1}} + \sum_{t:\omega_t<1} \|\Delta z_{t,a_t,b_t}^* \|_{\tilde{V}_{t-1}^{-1}} \\
 &\leq \sum_{t:\omega_t=1} \|\Delta z_{t,a_t,b_t}^* \|_{\tilde{V}_{t-1}^{-1}} + \frac{1}{\alpha} \sum_{t:\omega_t<1} \omega_t \|\Delta z_{t,a_t,b_t}^* \|_{\tilde{V}_{t-1}^{-1}} \|\Delta z_{t,a_t,b_t} \|_{\tilde{V}_{t-1}^{-1}} \\
 &\leq \sum_{t:\omega_t=1} \|\Delta z_{t,a_t,b_t}^* \|_{\tilde{V}_{t-1}^{-1}} + \frac{1}{\alpha} \left(\sum_{t:\omega_t<1} \omega_t \|\Delta z_{t,a_t,b_t}^* \|_{\tilde{V}_{t-1}^{-1}}^2 + \sum_{t:\omega_t<1} \omega_t \|\Delta z_{t,a_t,b_t} \|_{\tilde{V}_{t-1}^{-1}}^2 \right) \\
 &\leq \sum_{t:\omega_t=1} \|\Delta z_{t,a_t,b_t}^* \|_{\tilde{V}_{t-1}^{-1}} + \frac{\mathcal{C} + \mathcal{D}}{\sqrt{d}} \sum_{t:\omega_t<1} \|\omega_t^{1/2} \Delta z_{t,a_t,b_t}^* \|_{\tilde{V}_{t-1}^{-1}}^2 \\
 &\quad + \frac{\mathcal{C} + \mathcal{D}}{\sqrt{d}} \sum_{t:\omega_t<1} \|\omega_t^{1/2} \Delta z_{t,a_t,b_t} \|_{\tilde{V}_{t-1}^{-1}}^2. \tag{B.18}
 \end{aligned}$$

$\sum_{t:\omega_t<1} \|\omega_t^{1/2} \Delta z_{t,a_t,b_t} \|_{\tilde{V}_{t-1}^{-1}}^2$ is bounded as $\tilde{\mathcal{O}}(d)$ by a standard elliptic potential lemma (Lattimore & Szepesvári, 2020).

In the case of $\sum_{t:\omega_t<1} \|\omega_t^{1/2} \Delta z_{t,a_t,b_t}^* \|_{\tilde{V}_{t-1}^{-1}}^2$, we will use the generalized elliptic potential lemma:

By Lemma B.1, the upper bound of the potential sum depends on the choice of $p \in [0, 1]$. Note that the log-determinant term is bounded as $\log(\det \tilde{V}_T / \det \tilde{V}_0) = \mathcal{O}(d \log T)$, and the noise-dependent terms are independent of T . We apply the lemma for two specific cases:

- **Case 1** ($p = 1/2$): Substituting $p = 1/2$ into Lemma B.1, the leading term scales with $T^{1-1/2}(\mathcal{O}(d \log T))^{1/2} = \tilde{\mathcal{O}}(\sqrt{dT})$. Since the sum over a subset of indices $\{t : \omega_t = 1\}$ is bounded by the sum over all $t \in [T]$, we have:

$$\sum_{t:\omega_t=1} \|\Delta z_{t,a_t,b_t}^* \|_{\tilde{V}_{t-1}^{-1}} \leq \sum_{t=1}^T \|\Delta z_{t,a_t,b_t}^* \|_{\tilde{V}_{t-1}^{-1}} = \tilde{\mathcal{O}}(\sqrt{dT}). \tag{B.19}$$

ignoring logarithm terms and omitting sub-leading terms.

- **Case 2** ($p = 1$): Substituting $p = 1$, the leading term scales with $T^{1-1}(\mathcal{O}(d \log T))^1 = \tilde{\mathcal{O}}(d)$. Similarly, bounding the partial sum by the total sum yields:

$$\sum_{t:\omega_t<1} \|\Delta z_{t,a_t,b_t}^* \|_{\tilde{V}_{t-1}^{-1}}^2 \leq \sum_{t=1}^T \|\Delta z_{t,a_t,b_t}^* \|_{\tilde{V}_{t-1}^{-1}}^2 = \tilde{\mathcal{O}}(d). \tag{B.20}$$

ignoring logarithm terms and omitting sub-leading terms.

Combining Equations (B.17) to (B.20) and recalling that $\beta_T = \tilde{\mathcal{O}}(\sqrt{d} + \lambda M)$, the cumulative regret decomposes as:

$$2R_T = I_1 + I_2,$$

where:

$$I_1 := C_0(L_\Theta + \beta_T) \sqrt{d_x} \log(T/\delta) \sum_{t=1}^T t^{-\nu} = \tilde{\mathcal{O}}(\sqrt{d \cdot d_x} T^{1-\nu}),$$

$$I_2 := 3\beta_T \sum_{t=1}^T \|\Delta z_{t,a_t,b_t}^* \|_{\tilde{V}_{t-1}^{-1}} = \tilde{\mathcal{O}}(d\sqrt{T} + d(\mathcal{C} + \mathcal{D})).$$

Therefore, the total cumulative regret satisfies:

$$R_T = \tilde{\mathcal{O}}\left((d + \sqrt{d \cdot d_x})\sqrt{T} + d(\mathcal{C} + \mathcal{D})\right).$$

This completes the proof of Theorem 5.2. \square

C. Proof of Theorem 5.3

We adopt the piecewise linear link function $\sigma(x) = \frac{1}{2} + x$ for $x \in [-\frac{1}{2}, \frac{1}{2}]$. For any scaling factor $\kappa > 0$, we define the scaled link function as $\sigma_\kappa(x) := \sigma(\kappa x)$. Throughout this analysis, we assume that post-serving contexts are absent. We first introduce a fundamental lower bound that encapsulates both statistical variance and adversarial corruptions.

Lemma C.1 (Statistical and Corruption Lower Bound (Di et al., 2024, Theorem 5.4)). *For any learning algorithm \mathcal{A} , there exists an environment \mathcal{I}_1 such that the expected regret is lower-bounded as:*

$$\mathbb{E}[\text{Regret}(\mathcal{A}; \mathcal{I}_1)] \geq \Omega(d\sqrt{T} + dC),$$

where C denotes the total corruption budget.

To further account for the impact of feedback latency, we characterize the fundamental limits under an adversarial delay model.

Lemma C.2 (Adversarial Delay Lower Bound). *For any algorithm \mathcal{A} operating within an adversarial delay budget Λ , there exists an instance \mathcal{I}_2 such that:*

$$\mathbb{E}[\text{Regret}(\mathcal{A}; \mathcal{I}_2)] \geq \Omega(\sqrt{d\Lambda}).$$

Proof. We adopt the continuous action set construction from Di et al. (2024). Consider a parameter $\Theta_* \in \{-\Delta, +\Delta\}^d$ where each coordinate $\Theta_{*,i}$ is drawn i.i.d. uniformly at random, with $\Delta = 1/8$. The action set is defined as $\mathcal{A} = \{x \in \mathbb{R}^d : \|x\|_2 \leq 1\}$, and the utility function is linear in the parameter, i.e., $u(a) = \langle \Theta_*, a \rangle$ for any action $a \in \mathcal{A}$. Under this construction, the optimal action is given by $a^* = \frac{1}{\sqrt{d}} \text{sign}(\Theta_*)$, yielding an optimal utility of

$$u(a^*) = \left\langle \Theta_*, \frac{1}{\sqrt{d}} \text{sign}(\Theta_*) \right\rangle = \frac{1}{\sqrt{d}} \sum_{i=1}^d |\Theta_{*,i}| = \frac{1}{\sqrt{d}} \cdot d\Delta = \sqrt{d}\Delta. \quad (\text{C.21})$$

We now describe the adversary's delay assignment strategy. Define

$$M = \left\lfloor \frac{-1 + \sqrt{1 + 8\Lambda}}{2} \right\rfloor = \Theta(\sqrt{\Lambda}), \quad (\text{C.22})$$

which corresponds to the largest integer satisfying $\frac{M(M+1)}{2} \leq \Lambda$. The adversary assigns delay $\tau_t = M - t + 1$ to round t for all $t \in [M]$, ensuring that all feedback is withheld until after round M . This creates a blind phase during which the learner receives no information.

It remains to analyze the regret incurred during this blind phase. In the dueling bandits framework, the learner selects two actions (a_t, b_t) at each round, and the per-round regret is defined as

$$\text{Regret}_t = (u(a^*) - u(a_t)) + (u(a^*) - u(b_t)), \quad (\text{C.23})$$

which measures the suboptimality of both selected actions relative to the optimal action a^* .

For each round $t \in [M]$, the learner operates with an empty history $\mathcal{H}_t = \emptyset$. Since the learner has received no feedback, the actions a_t and b_t are chosen independently of the true parameter Θ_* . By the symmetry of the prior distribution, each coordinate satisfies $\mathbb{E}[\Theta_{*,i}] = \frac{1}{2}(+\Delta) + \frac{1}{2}(-\Delta) = 0$, which implies $\mathbb{E}[\Theta_*] = \mathbf{0}$. Consequently, for any action a_t that is independent of Θ_* , we have

$$\mathbb{E}[u(a_t)] = \mathbb{E}[\langle \Theta_*, a_t \rangle] = \langle \mathbb{E}[\Theta_*], a_t \rangle = \langle \mathbf{0}, a_t \rangle = 0. \quad (\text{C.24})$$

By the same argument, $\mathbb{E}[u(b_t)] = 0$. Therefore, the expected per-round regret is

$$\mathbb{E}[\text{Regret}_t] = 2u(a^*) - \mathbb{E}[u(a_t)] - \mathbb{E}[u(b_t)] = 2\sqrt{d}\Delta - 0 - 0 = 2\sqrt{d}\Delta. \quad (\text{C.25})$$

Aggregating over all M rounds in the blind phase yields

$$\mathbb{E}[\text{Regret}] \geq \sum_{t=1}^M \mathbb{E}[\text{Regret}_t] = M \cdot 2\sqrt{d}\Delta = \Omega(\sqrt{\Lambda} \cdot \sqrt{d}) = \Omega(\sqrt{d\Lambda}), \quad (\text{C.26})$$

which completes the proof. \square

Lemma C.3 (Stochastic Delay Lower Bound). *For any algorithm \mathcal{A} with stochastic delays of mean μ_τ , there exists an instance \mathcal{I}_3 such that*

$$\mathbb{E}[\text{Regret}(\mathcal{A}; \mathcal{I}_3)] \geq \Omega(d\mu_\tau). \quad (\text{C.27})$$

Proof. Consider the deterministic delay distribution $\tau_t = \mu_\tau$ for all t , which trivially satisfies $\mathbb{E}[\tau] = \mu_\tau$. Let $\Theta_* \in \{-\Delta, +\Delta\}^d$ where each coordinate $\Theta_{*,i}$ is drawn i.i.d. uniformly at random, with $\Delta = 1/4$. The action set is defined as the hypercube $\mathcal{A} = \{-1, 1\}^d$, and the utility function is linear in the parameter, i.e., $u(a) = \langle \Theta_*, a \rangle = \sum_{i=1}^d a_i \Theta_{*,i}$ for any action $a \in \mathcal{A}$. Under this construction, the optimal action is $a^* = \text{sign}(\Theta_*)$, which matches the sign of each coordinate precisely, yielding an optimal utility of

$$u(a^*) = \sum_{i=1}^d \text{sign}(\Theta_{*,i}) \cdot \Theta_{*,i} = \sum_{i=1}^d |\Theta_{*,i}| = d\Delta. \quad (\text{C.28})$$

For all rounds $t \leq \mu_\tau$, the learner operates with an empty history $\mathcal{H}_t = \emptyset$, creating a blind phase during which no feedback is available. Since the learner has received no information, the actions a_t and b_t are chosen independently of the true parameter Θ_* . By the symmetry of the prior distribution, each coordinate satisfies $\mathbb{E}[\Theta_{*,i}] = \frac{1}{2}(+\Delta) + \frac{1}{2}(-\Delta) = 0$, which implies $\mathbb{E}[\Theta_*] = \mathbf{0}$. Consequently, for any action a_t that is independent of Θ_* , we have

$$\mathbb{E}[u(a_t)] = \mathbb{E}[\langle \Theta_*, a_t \rangle] = \langle \mathbb{E}[\Theta_*], a_t \rangle = \langle \mathbf{0}, a_t \rangle = 0. \quad (\text{C.29})$$

By the same argument, $\mathbb{E}[u(b_t)] = 0$. In the dueling bandits framework, the learner selects two actions (a_t, b_t) at each round, and the expected per-round regret is

$$\mathbb{E}[\text{Regret}_t] = 2u(a^*) - \mathbb{E}[u(a_t)] - \mathbb{E}[u(b_t)] = 2d\Delta - 0 - 0 = 2d\Delta. \quad (\text{C.30})$$

Aggregating over all μ_τ rounds in the blind phase yields

$$\mathbb{E}[\text{Regret}] \geq \sum_{t=1}^{\mu_\tau} \mathbb{E}[\text{Regret}_t] = \mu_\tau \cdot 2d\Delta = \Omega(d\mu_\tau), \quad (\text{C.31})$$

which completes the proof. \square

Proof of Theorem 5.3. By Lemmas C.1–C.3, for any algorithm \mathcal{A} , we have

$$\sup_{\mathcal{I}} \mathbb{E}[\text{Regret}(\mathcal{A}; \mathcal{I})] \geq \max \left\{ \Omega(d\sqrt{T} + dC), \Omega(\sqrt{d\Lambda}), \Omega(d\mu_\tau) \right\}. \quad (\text{C.32})$$

Since adversarial and stochastic delays are mutually exclusive, and using the inequality $\max(A, B) \geq (A + B)/2$, we obtain

$$\sup_{\mathcal{I}} \mathbb{E}[\text{Regret}(\mathcal{A}; \mathcal{I})] \geq \Omega \left(d\sqrt{T} + dC + \max\{\sqrt{d\Lambda}, d\mu_\tau\} \right). \quad (\text{C.33})$$

Finally, for any $\kappa > 0$, consider the scaled link function $\sigma_\kappa(x) = \sigma(\kappa x)$. By the same scaling argument as in Di et al. (2024, Theorem 5.4), the lower bound becomes $\Omega \left((d\sqrt{T} + dC + \max\{\sqrt{d\Lambda}, d\mu_\tau\})/\kappa \right)$. \square

Remark C.4 (Different Constructions). The adversarial delay bound uses the continuous action set $\{x : \|x\|_2 \leq 1\}$, while the stochastic delay bound uses the discrete set $\{e_i\}_{i=1}^d$. This is because:

- Adversarial delays can concentrate budget to create a blind phase of length $\Theta(\sqrt{\Lambda})$, and the continuous set yields per-round regret $\Theta(\sqrt{d})$, giving $\Omega(\sqrt{d\Lambda})$.
- Stochastic delays create a fixed blind phase of length μ_τ , and the discrete set with d sub-instances yields $\Omega(d\mu_\tau)$ via minimax over coordinates.

Since these are different instances combined via minimax, both bounds are valid.

Remark C.5 (On the Nature of the Lower Bound). Our lower bound is established via the standard minimax framework, where different terms may arise from different hard instances. This is consistent with prior works (Di et al., 2024; He et al., 2022; Gupta et al., 2019). The additive form $\Omega(A + B + C)$ follows from $\max(A, B, C) \geq (A + B + C)/3$, which is the standard way to express minimax lower bounds in the bandit literature.

Remark C.6 (On the Additive Form). The lower bound is established via the standard minimax framework following Di et al. (2024); He et al. (2022); Gupta et al. (2019). Different terms arise from different hard instance families:

- $\Omega(d\sqrt{T}/\kappa)$: Statistical complexity from continuous action set with $\Delta = \Theta(\sqrt{d/T})$
- $\Omega(dC/\kappa)$: Corruption cost from discrete action set with d sub-instances
- $\Omega(\sqrt{d\Lambda}/\kappa)$ or $\Omega(d\mu_\tau/\kappa)$: Delay cost from blind phase construction

D. Experimental Details

D.1. Implementation Details

Table D.1. Summary of Experimental Settings and Hyperparameters.

Parameter	Symbol	Value
<i>Environment</i>		
Time Horizon	T	2,000
Pre-serving Dimension	d_x	10
Number of Arms	K	10
Number of Runs	-	5
<i>Robustness Settings</i>		
Corruption Budget	\mathcal{C}	25
Strategic Delay Budget	Λ	10,000
Stochastic Delay Mean	μ_τ	100
Stochastic Delay Std	σ	10
<i>Algorithm Hyperparameters</i>		
Regularization	λ	1.0
MLP Hidden Units	-	(64, 64)
MLP Learning Rate	η	10^{-3}
Optimizer	Adam (Kingma, 2014)	

In Section 6, we empirically evaluate the performance of our proposed method, RCDP-UCB, alongside baseline algorithms within a synthetic contextual dueling bandit framework. The dimension of the pre-serving context was set to $d_x = 10$. At each round t , the environment generates a pool of $K = 10$ arms. The ground-truth parameters $\Theta^* \in \mathbb{R}^d$ were sampled from a standard normal distribution and normalized to ensure valid utility scales. To investigate the method’s adaptability to complex environmental dynamics, we tested four distinct mapping functions $\phi : \mathcal{X} \rightarrow \mathcal{Y}$ governing the relationship between pre-serving and post-serving contexts: *Polynomial*, *Absolute*, *Cosine*, and *Sinusoidal*. To verify the robustness of our method against data irregularities, we introduced both adversarial corruptions and feedback delays. The environment was constrained by a corruption budget of $\mathcal{C} = 25$ and a strategic delay budget of $\Lambda = 10,000$. Additionally, stochastic delays were modeled with a mean of $\mu_\tau = 100$ and a standard deviation of $\sigma = 10$. For the neural network approximation, we employed a Multi-Layer Perceptron (MLP) consisting of two hidden layers with 64 units each (with the ReLU activation). The network was optimized using Adam (Kingma, 2014) with a learning rate of $\eta = 10^{-3}$ and a regularization coefficient of $\lambda = 1.0$. The experiments were conducted over a time horizon of $T = 2,000$ rounds, and all reported results were averaged over 5 independent runs with different random seeds to ensure statistical reliability. The network was optimized using Adam with a learning rate of 10^{-3} and trained for 2 epochs per update. Regarding the bandit hyperparameters, we set the regularization parameter to $\lambda = 1.0$.

A comprehensive summary of the experimental configurations and hyperparameters is provided in Table D.1.

All experiments were conducted on a workstation equipped with an AMD Ryzen 9 9950X3D 16-Core Processor and 48GB of RAM. The algorithms were implemented in Python 3.10, utilizing PyTorch for the neural network components and NumPy for vector operations. The experiments were executed in a CPU-only environment, as the computational overhead of the multi-layer perceptron (MLP) utilized for context mapping was negligible, and no GPU acceleration was required.

D.2. Related Algorithms for Contextual Dueling Bandits

We review four representative algorithms for the contextual dueling bandit problem: RCDB, COLSTIM, MaxInP, and MaxPair-UCB. All these algorithms assume a linear relationship between the context-action features and the latent utility or reward.

RCDB (Robust Contextual Dueling Bandits). Proposed by Di et al. (2024), RCDB is designed to handle adversarial feedback where a strong adversary may flip the preference labels. To mitigate the impact of malicious feedback, RCDB employs an *uncertainty-weighted Maximum Likelihood Estimator (MLE)*. The estimator $\hat{\theta}_t$ is obtained by solving the weighted score equation:

$$\lambda\theta + \sum_{\tau=1}^{t-1} w_{\tau}(\sigma(\phi_{\tau}^{\top}\theta) - o_{\tau})\phi_{\tau} = 0, \quad (\text{D.34})$$

where $\phi_{\tau} = \phi(x_{\tau}, a_{\tau}) - \phi(x_{\tau}, b_{\tau})$ denotes the differential feature vector, and o_{τ} is the observed feedback. The key innovation lies in the uncertainty-dependent weights $w_{\tau} = \min\{1, \alpha/\|\phi_{\tau}\|_{\Sigma_{\tau}^{-1}}\}$, which down-weight samples with high uncertainty to limit the adversary's influence. The algorithm selects the arm pair (a_t, b_t) that maximizes a robust Upper Confidence Bound (UCB) objective:

$$(a_t, b_t) = \operatorname{argmax}_{a, b \in \mathcal{A}_t} \left\{ (\phi(x_t, a) + \phi(x_t, b))^{\top} \hat{\theta}_t + \beta_t \|\phi(x_t, a) - \phi(x_t, b)\|_{\Sigma_t^{-1}} \right\}. \quad (\text{D.35})$$

COLSTIM (CoLST Imitator). Introduced by (Bengs et al., 2022), COLSTIM operates under the Linear Stochastic Transitivity (LST) model. It adopts a randomized exploration strategy that imitates the underlying feedback process. Specifically, at each round t , it generates perturbed utility estimates for each arm a by adding noise scaled by the confidence width:

$$\tilde{u}_{t,a} = x_{t,a}^{\top} \hat{\theta}_t + \epsilon_{t,a} \|x_{t,a}\|_{M_t^{-1}}, \quad (\text{D.36})$$

where $\epsilon_{t,a}$ is a random perturbation sampled from a specific distribution (e.g., Gumbel) and M_t is the Gram matrix. The first arm a_t is chosen to maximize this perturbed utility, $\tilde{u}_{t,a}$. The second arm b_t is then selected as the *toughest competitor* to a_t , maximizing the optimistic pairwise difference:

$$b_t = \operatorname{argmax}_{b \in \mathcal{A}_t} \left((x_{t,b} - x_{t,a_t})^{\top} \hat{\theta}_t + c_t \|x_{t,b} - x_{t,a_t}\|_{M_t^{-1}} \right). \quad (\text{D.37})$$

MaxInP (Maximum Informative Pair). Developed by (Saha, 2021), MaxInP focuses on efficient exploration by maintaining a set of “promising” arms, \mathcal{C}_t , which contains arms that are plausibly the best with high probability. The algorithm avoids playing suboptimal arms by restricting selection to \mathcal{C}_t . Within this set, it selects the pair (a_t, b_t) that maximizes the information gain, quantified by the variance of the pairwise difference:

$$(a_t, b_t) = \operatorname{argmax}_{a, b \in \mathcal{C}_t} \|\phi(x_t, a) - \phi(x_t, b)\|_{V_t^{-1}}, \quad (\text{D.38})$$

where V_t is the covariance matrix of the differential features. This *max-variance* strategy ensures that the algorithm continually reduces uncertainty in the directions most relevant to distinguishing the best arms.

MaxPair-UCB. As discussed in (Di et al., 2023), MaxPair-UCB is a UCB-based algorithm that simplifies the selection process of MaxInP by eliminating the explicit construction of a promising set. Instead, it directly selects the pair that maximizes an optimistic estimate of the sum-reward combined with an exploration bonus on the pairwise difference. The selection rule is given by:

$$(a_t, b_t) = \operatorname{argmax}_{a, b \in \mathcal{A}_t} \left\{ (x_{t,a} + x_{t,b})^{\top} \hat{\theta}_t + \beta_t \|x_{t,a} - x_{t,b}\|_{\Sigma_t^{-1}} \right\}. \quad (\text{D.39})$$

This approach naturally balances exploitation (maximizing the estimated sum score $(x_{t,a} + x_{t,b})^\top \hat{\theta}_t$) and exploration (maximizing the pairwise uncertainty $\|x_{t,a} - x_{t,b}\|_{\Sigma_t^{-1}}$), and serves as a strong baseline in variance-aware and adversarial settings.

D.3. Implementation with PyTorch.

Listing 1 demonstrates a simplified PyTorch implementation of our proposed algorithm, RCDP-UCB. The class integrates the online learning of the post-serving context mapping with the robust bandit strategy. To approximate the unknown mapping, a neural network is employed and trained online via the `train_mapping` method, which updates the model using collected context-outcome pairs. The `get_features` method then concatenates the original context with the network’s prediction to form the augmented feature vector used for decision-making. In the `select_arms` method, we employ an adaptive UCB strategy that relies on the *Observed History* matrix (`self.W_inv`) to construct confidence bounds based on actual localized information. Critically, robustness is enforced by the `get_weight` method, which computes a down-weighting factor using the *Full History* matrix (`self.V_inv`). This ensures that updates with high forward-looking uncertainty are throttled before they can destabilize the model in the `update` step, effectively neutralizing the impact of potential strategic delays or corruptions.

```
class RCDP_UCB(nn.Module):
    def __init__(self, dim, alpha=0.5, lambda_reg=1.0, c_t=1.0, kappa=0.1):
        super().__init__()
        self.kappa = kappa
        self.dim = dim
        self.theta_hat = torch.zeros(dim)

        # Full History Matrix V (for Selection & Weighting)
        self.V_inv = (1.0 / lambda_reg) * torch.eye(dim)

        # Observed History Matrix W (for Gradient Update)
        self.W_inv = (1.0 / lambda_reg) * torch.eye(dim)

        self.alpha = alpha
        self.c_t = c_t

    def select_arms(self, Z):
        """
        Z: Features including predicted post-serving context (K, dim)
        Returns: a_t, b_t, omega_t
        """
        # 1. Champion (Greedy)
        utilities = Z @ self.theta_hat
        a_t = torch.argmax(utilities)
        z_a = Z[a_t]

        # 2. Challenger (Use V_inv for Optimism in Face of Uncertainty)
        Delta_Z = Z - z_a
        mean_diff = Delta_Z @ self.theta_hat

        # KEY: Use V_inv (Full History) for Confidence Width
        width_V = torch.sqrt(torch.sum((Delta_Z @ self.V_inv) * Delta_Z, dim=1))

        scores_b = mean_diff + self.c_t * width_V
        b_t = torch.argmax(scores_b)

        # 3. Calculate Robust Weight (omega_t)
        delta_z = Z[a_t] - Z[b_t]
        norm_V = torch.sqrt(delta_z @ self.V_inv @ delta_z)

        if norm_V < 1e-9:
            omega_t = 1.0
        else:
            omega_t = min(1.0, self.alpha / norm_V)
```

```

# 4. Phantom Update of V (Full History)
# We update V immediately to reflect the "commitment" to this arm pair
# Formula: V <- V + kappa * omega_t * outer(delta, delta)
# Using Sherman-Morrison for V_inv
v_vec = torch.sqrt(self.kappa * omega_t) * delta_z
Av = self.V_inv @ v_vec
denom = 1 + torch.dot(v_vec, Av)
self.V_inv -= torch.outer(Av, Av) / denom

return a_t, b_t, omega_t

def update(self, delta_z, outcome, omega_t):
    """
    Real Update when Feedback Arrives
    """
    # 1. Update Observed Matrix W using Robust Weight
    w_vec = torch.sqrt(self.kappa * omega_t) * delta_z
    Aw = self.W_inv @ w_vec
    denom_w = 1 + torch.dot(w_vec, Aw)
    self.W_inv -= torch.outer(Aw, Aw) / denom_w

    # 2. Weighted Gradient Step
    mu_val = torch.sigmoid(torch.dot(self.theta_hat, delta_z))

    # Gradient direction weighted by omega_t * W_inv
    step = self.W_inv @ (omega_t * (outcome - mu_val) * delta_z)
    self.theta_hat += step

```

Listing 1. PyTorch Implementation of RCDP-UCB (Simplified)

E. Additional Experiments

E.1. Experiments on Real-world Datasets

We validate the robustness and scalability of RCDP-UCB using eight diverse classification datasets from the UCI Machine Learning Repository and OpenML. For each dataset, we partition the feature vector into visible pre-serving contexts (\mathbf{x}_t) and latent post-serving features (\mathbf{y}_t), as summarized in Table E.2.

Dataset Preparation. In each round t , the environment randomly samples $K = 30$ instances from the dataset to form the available set of arms \mathcal{A}_t . The ground-truth utility of an arm is defined by its class label $c \in \{0, \dots, C - 1\}$, where higher-indexed classes are considered preferable. All feature values are standardized using zero-mean and unit variance before the start of the simulation.

Empirical Results. Figure E.1 shows the results for three representative datasets: Magic Gamma Telescope ($d = 6$), Statlog ($d = 20$), and Spambase ($d = 30$). Across all datasets and both delay regimes (strategic starvation and stochastic network latency), RCDP-UCB consistently outperforms robust and non-robust baselines. Notably, even on real-world distributions where the linear preference assumption is only an approximation, RCDP-UCB’s weighting mechanism effectively mitigates the bias introduced by the combination of adversarial corruption and delayed feedback.

Table E.2. Statistics of real-world datasets used in the experiments. The feature vectors are split into pre-serving d -dim and post-serving e -dim components. Utility is defined by class labels.

Dataset	Samples	Total Features	Pre (d)	Post (e)	Classes
Magic	19,020	10	6	4	2
Statlog (Satimage)	6,430	36	20	16	6
Spambase	4,601	57	30	27	2

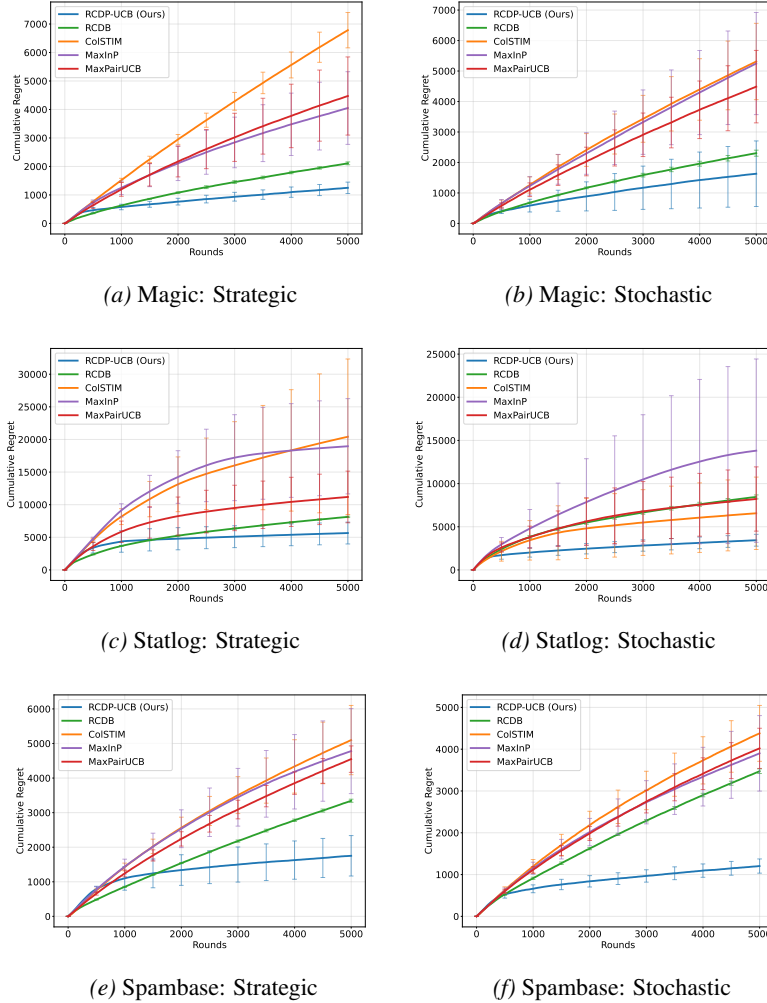


Figure E.1. **Real-world Dataset Results:** Cumulative regret comparison on Magic, Statlog, and Spambase datasets under adversarial corruption ($\mathcal{C} = 25$), strategic delays ($\Lambda = 10,000$), and stochastic delays ($\mu_\tau = 100$). All experiments were conducted across 5 runs with random seeds.

E.2. Increasing Context Dimension

In this section, we provide an extensive empirical evaluation of RCDP-UCB across varying pre-serving context dimensions $d_x \in \{10, 20, 30\}$. We investigate two scenarios: with and without post-serving learning.

Sensitivity without Baseline Post-Serving Learning. Figure E.2 illustrates the performance scaling with respect to dimension d in the linear task using only pre-serving features. RCDP-UCB maintains robust sublinear regret across all dimensions, with the performance gap relative to RCDB widening as d increases. This validates the efficacy of our weighting mechanism in high-dimensional settings under joint $\mathcal{C} + \mathcal{D}$ perturbations.

Sensitivity with Baseline Post-Serving Learning. We further evaluate robustness across all three mappings (Absolute, Polynomial, and Sinusoidal) when all baselines are equipped with MLP-based post-serving learning (Figure E.3, Figure E.4, Figure E.5). Even with the additional information provided by $\hat{\phi}_t$, standard baselines suffer from the unified impact of corruption and delay. RCDP-UCB consistently maintains superior performance, demonstrating that its advantage stems from the adaptive information-weighted estimation rather than mere feature engineering. The stability across Absolute, Polynomial, and Sinusoidal tasks confirms the algorithm’s versatility in handling diverse latent dynamics as the complexity of the feature manifold increases.

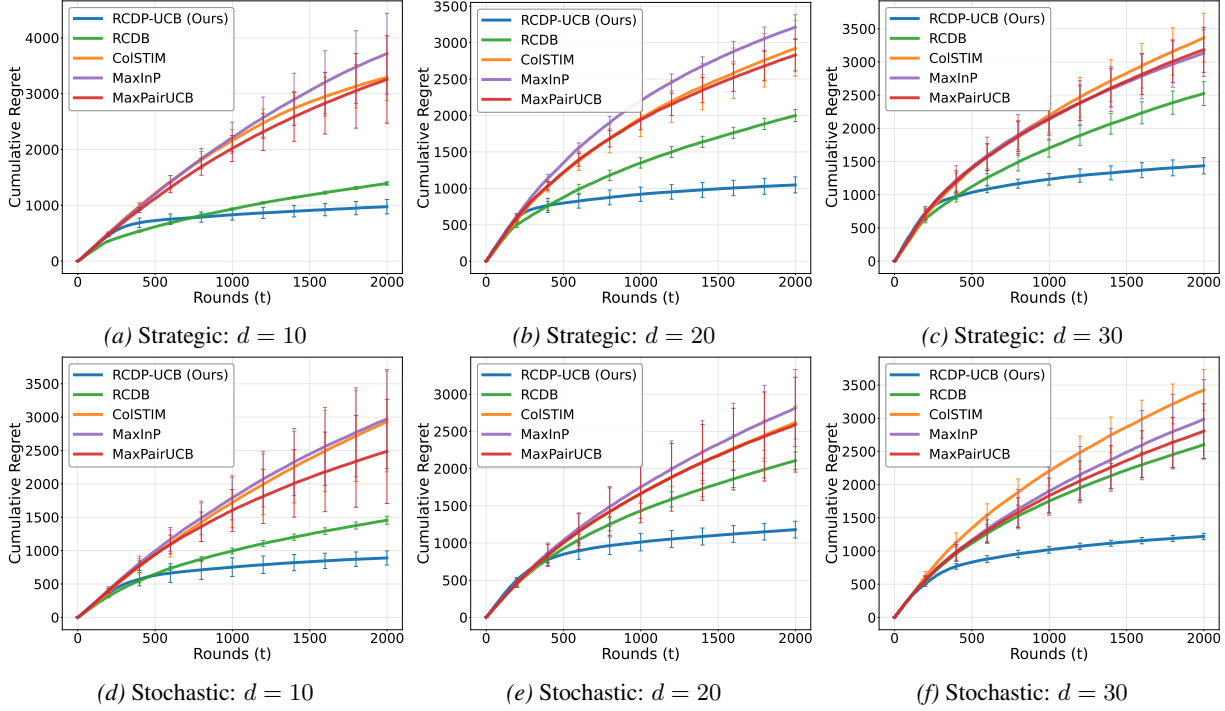


Figure E.2. **Linear Problem (Pre-serving Baselines):** Cumulative regret with increasing context dimension d under adversarial corruption ($\mathcal{C} = 25$), strategic delays ($\Lambda = 10, 000$), and stochastic delays ($\mu_\tau = 100$). All experiments were conducted across 5 runs with random seeds.

E.3. Increasing Action Dimension

We examine the scalability of RCDP-UCB as the number of available arms K increases from 10 to 30. Similar to the context dimension analysis, we consider both pre-serving and post-serving baseline scenarios.

Sensitivity without Baseline Post-Serving Learning. Figure E.6 illustrates the performance scaling with respect to the number of arms K in the linear task. RCDP-UCB maintains stable sublinear regret as K increases, consistently outperforming RCDB and other competitive baselines. These results underscore the robustness of our proposed framework under concurrent adversarial corruptions and feedback delays.

Sensitivity with Baseline Post-Serving Learning. The robustness of RCDP-UCB is further validated across Absolute, Polynomial, and Sinusoidal mappings when all baselines incorporate post-serving learning (Figure E.7, Figure E.8, Figure E.9). Even with the ability to predict latent contexts, baselines struggle to maintain low regret as the action space expands. In contrast, the performance of RCDP-UCB remains remarkably consistent. This suggests that the adaptive weighting mechanism effectively controls the variance of the MLE estimation, preventing the combined noise of corruption and delay from overwhelming the identification of the optimal arm even as the competition among arms increases.

E.4. Varying Corruption Budget

We investigate the robustness of RCDP-UCB as the total budget of adversarial corruption \mathcal{C} varies. Specifically, we test $\mathcal{C} \in \{10, 15, 20\}$ under a fixed mean stochastic delay $\mu_\tau = 100$, standard deviation $\sigma = 10$.

Empirical Analysis. Figure E.10 shows the cumulative regret for the linear problem with context dimensions $d = 10$ and $d = 20$. As the corruption budget increases, the bias introduced by the adversary becomes more significant. However, RCDP-UCB consistently maintains lower regret and faster convergence compared to both robust and non-robust baselines. This is achieved through the weighted MLE framework, where the influence of potentially corrupted observations is balanced by the information gain weights ω_t and the corruption-aware parameter estimation, ensuring that the learner remains effective even when a portion of the preferences are manipulated.

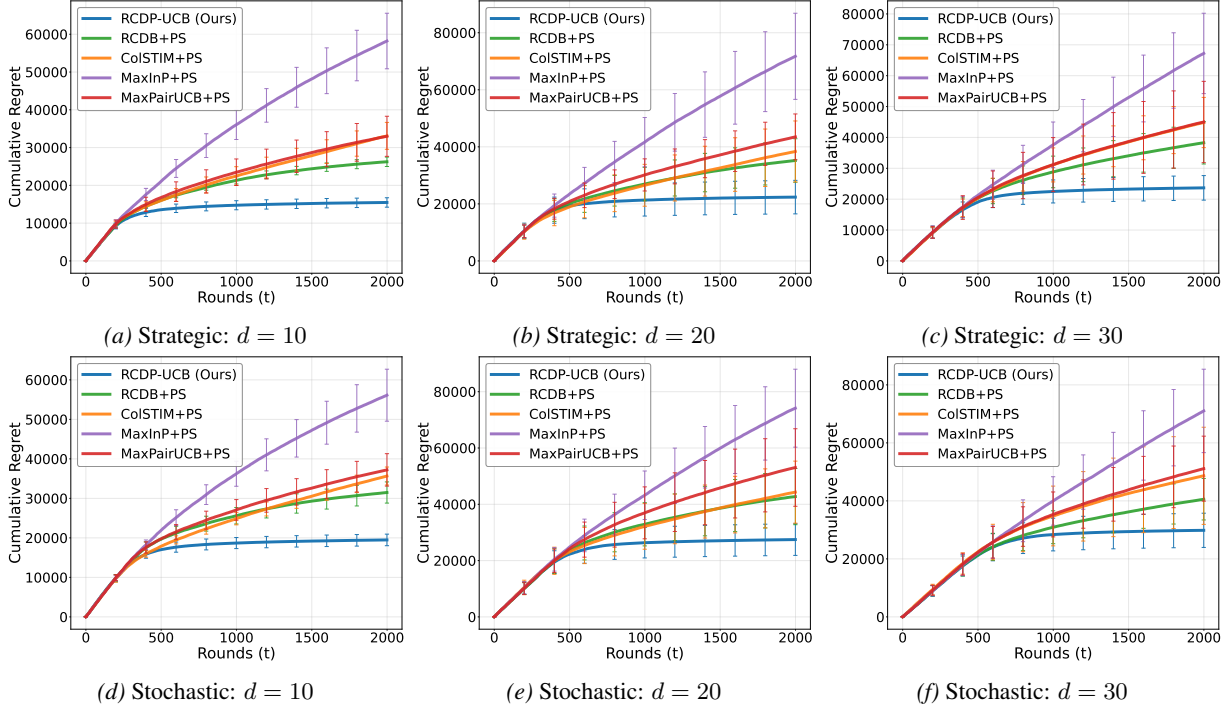


Figure E.3. **Absolute Mapping (Post-serving Learning):** Cumulative regret with increasing context dimension d under adversarial corruption ($\mathcal{C} = 25$), strategic delays ($\Lambda = 10,000$), and stochastic delays ($\mu_\tau = 100$), where all baselines learn ϕ_* . All experiments were conducted across 5 runs with random seeds.

E.5. Varying Total Budget of Adversarial Delay and Mean of Sub-Gaussian Delay

We analyze the performance of RCDP-UCB as the severity of feedback delays increases. Specifically, we vary the strategic delay budget Λ from 3,600 to 10,000 and the mean of stochastic sub-Gaussian delays μ_τ from 60 to 100.

Sensitivity without Baseline Post-Serving Learning. Figure E.11 summarizes the cumulative regret for the linear task. As the delay budget or mean delay increases, the learner receives feedback less frequently, leading to slower parameter convergence. RCDP-UCB demonstrates superior robustness compared to robust baselines like RCDB, maintaining lower regret even under severe starvation attacks.

Sensitivity with Baseline Post-Serving Learning. The robustness is further evaluated across Absolute, Polynomial, and Sinusoidal mappings where all baselines are augmented with post-serving learning (Figure E.12, Figure E.13, Figure E.14). RCDP-UCB consistently outperforms the baselines across all delay levels and mappings. The adaptive weighting mechanism in RCDP-UCB ensures that even when delays are large, the parameter updates are properly normalized by the local information density (captured by ω_t), allowing for robust learning where standard MLE-based approaches struggle.

E.6. Increasing STD. of Sub-Gaussian Delay

We assess the sensitivity of RCDP-UCB to the variance of stochastic delays by varying variance σ^2 from 0 to 150, while fixing the mean delay $\mu_\tau = 100$ and corruption budget $\mathcal{C} = 25$. Figure E.15 illustrates that the cumulative regret of RCDP-UCB remains remarkably stable across all evaluated noise levels. This empirical evidence validates that RCDP-UCB is robust to both the expected magnitude and the stochastic fluctuations of delays, a result consistent with the theoretical bounds established in Theorems 5.2 and 5.3.

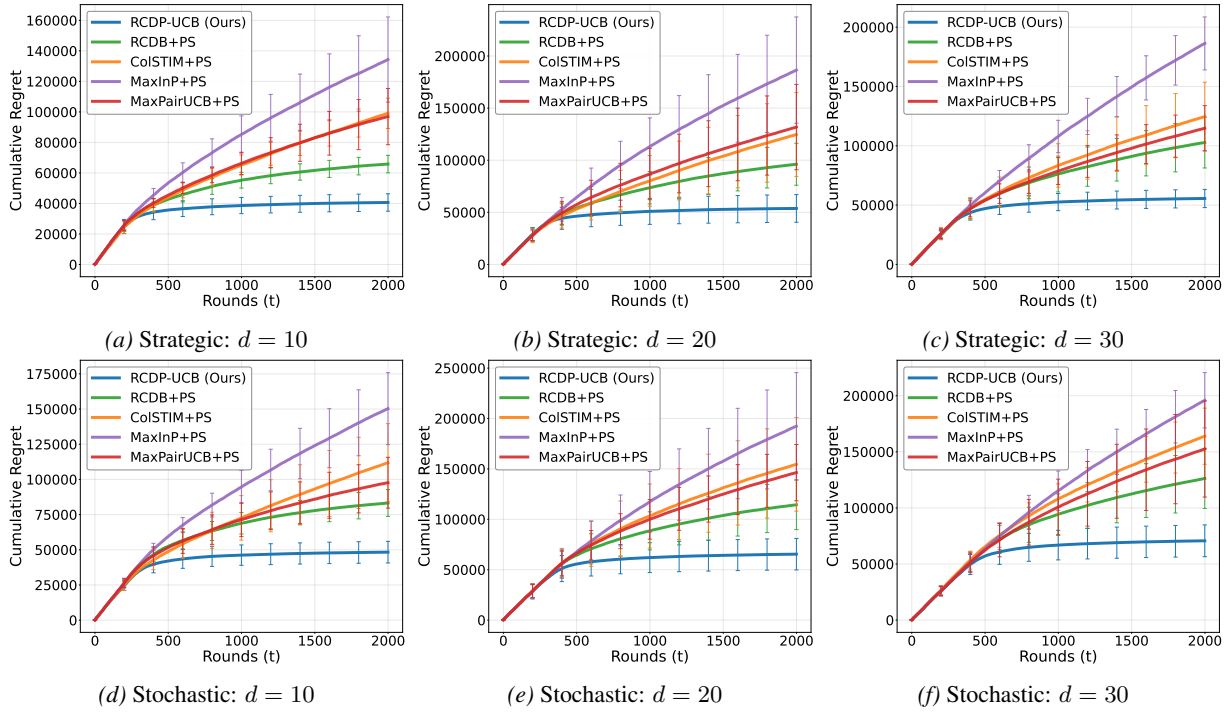


Figure E.4. **Polynomial Mapping (Post-serving Learning)**: Cumulative regret with increasing context dimension d under adversarial corruption ($C = 25$), strategic delays ($\Lambda = 10, 000$), and stochastic delays ($\mu_\tau = 100$), where all baselines learn ϕ_* . All experiments were conducted across 5 runs with random seeds.

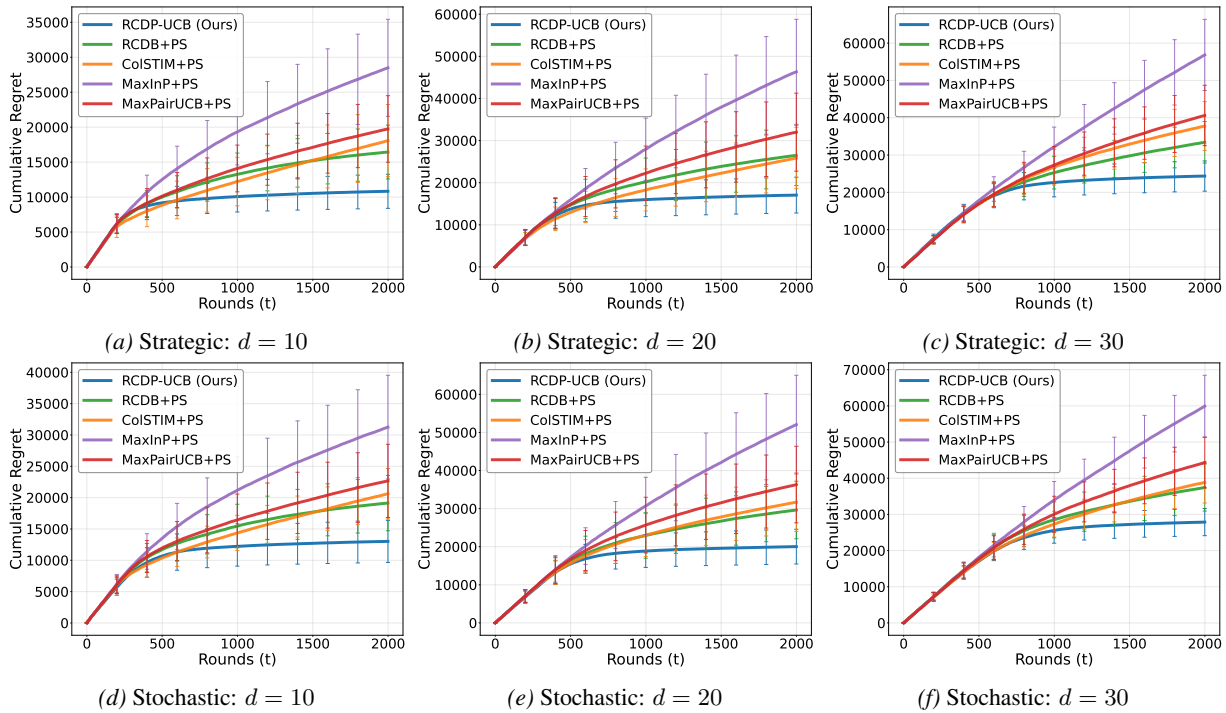


Figure E.5. **Sinusoidal Mapping (Post-serving Learning)**: Cumulative regret with increasing context dimension d under adversarial corruption ($C = 25$), strategic delays ($\Lambda = 10, 000$), and stochastic delays ($\mu_\tau = 100$), where all baselines learn ϕ_* . All experiments were conducted across 5 runs with random seeds.

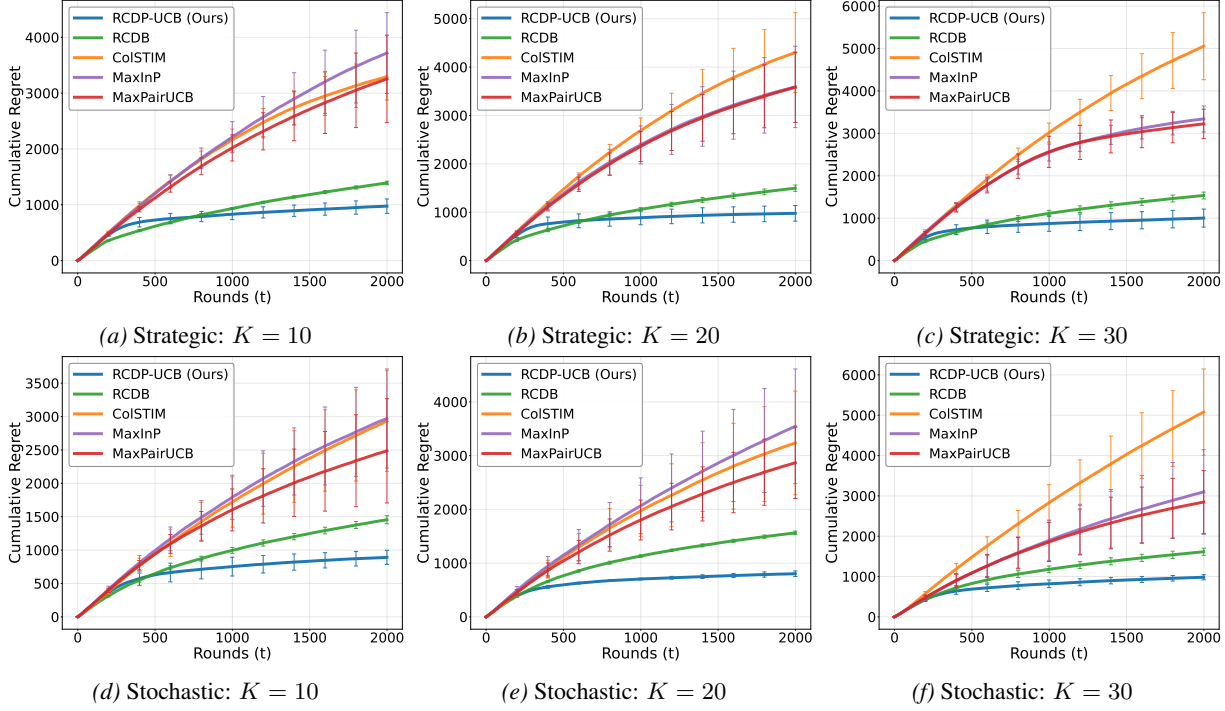


Figure E.6. **Polynomial Mapping (Pre-serving Baselines)**: Cumulative regret with increasing number of arms K under adversarial corruption ($\mathcal{C} = 25$), strategic delays ($\Lambda = 10, 000$), and stochastic delays ($\mu_\tau = 100$). All experiments were conducted across 5 runs with random seeds.

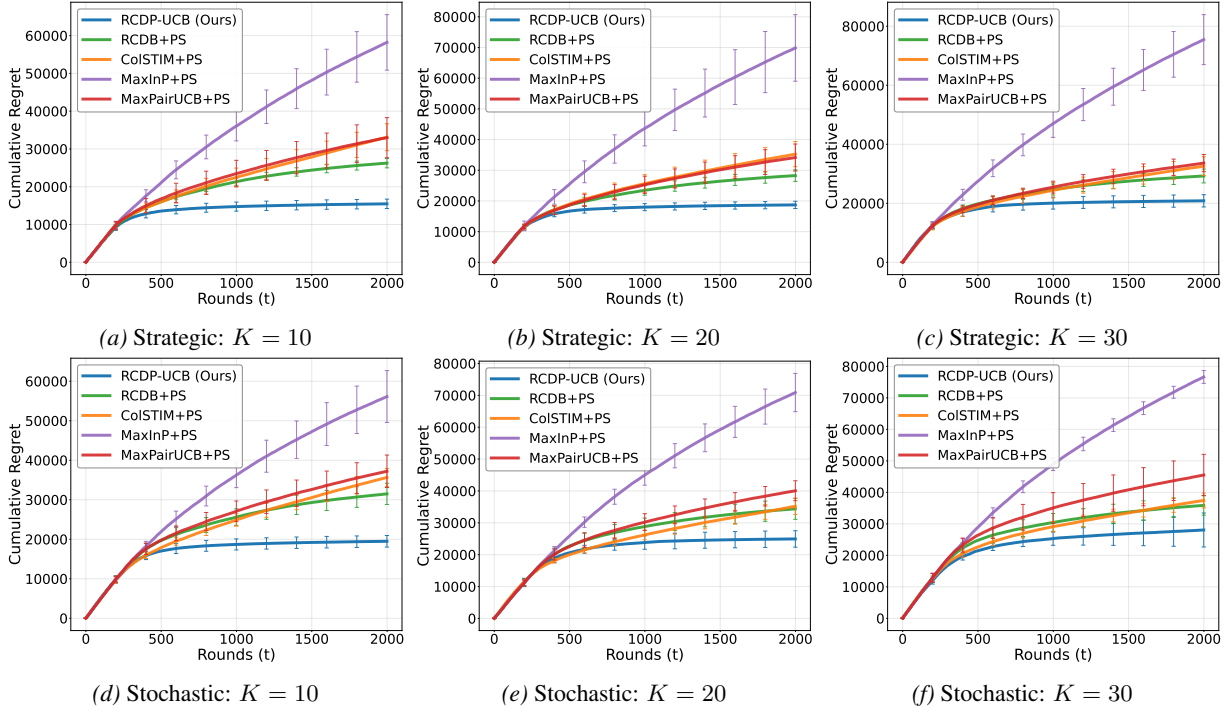


Figure E.7. **Absolute Mapping (Post-serving Learning)**: Cumulative regret with increasing number of arms K under adversarial corruption ($\mathcal{C} = 25$), strategic delays ($\Lambda = 10, 000$), and stochastic delays ($\mu_\tau = 100$), where all baselines learn ϕ_* . All experiments were conducted across 5 runs with random seeds.

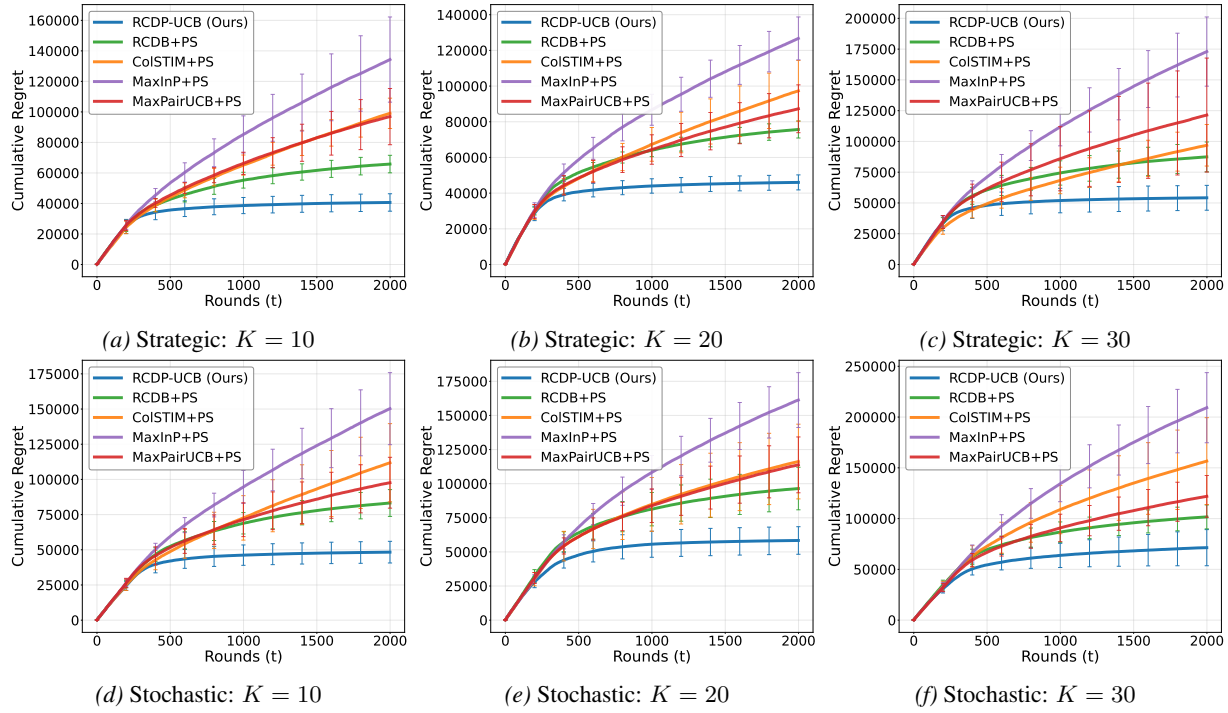


Figure E.8. **Polynomial Mapping (Post-serving Learning)**: Cumulative regret with increasing number of arms K under adversarial corruption ($C = 25$), strategic delays ($\Lambda = 10, 000$), and stochastic delays ($\mu_\tau = 100$), where all baselines learn ϕ_* . All experiments were conducted across 5 runs with random seeds.

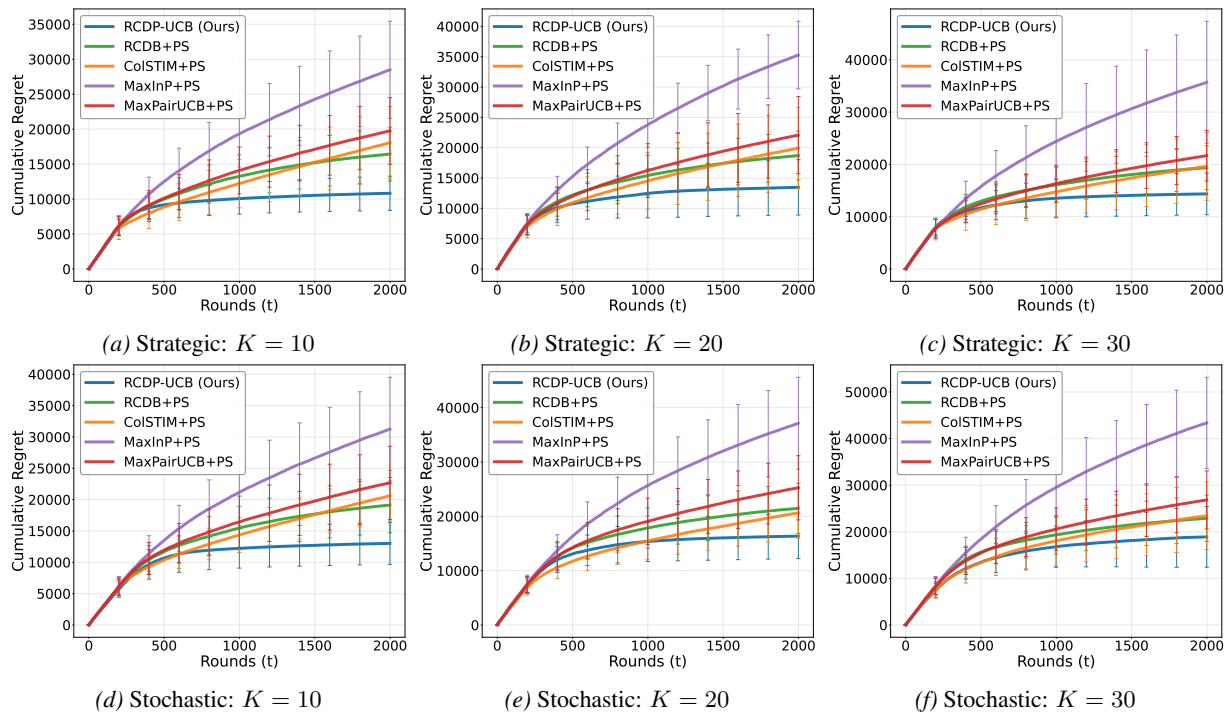


Figure E.9. **Sinusoidal Mapping (Post-serving Learning)**: Cumulative regret with increasing number of arms K under adversarial corruption ($C = 25$), strategic delays ($\Lambda = 10, 000$), and stochastic delays ($\mu_\tau = 100$), where all baselines learn ϕ_* . All experiments were conducted across 5 runs with random seeds.

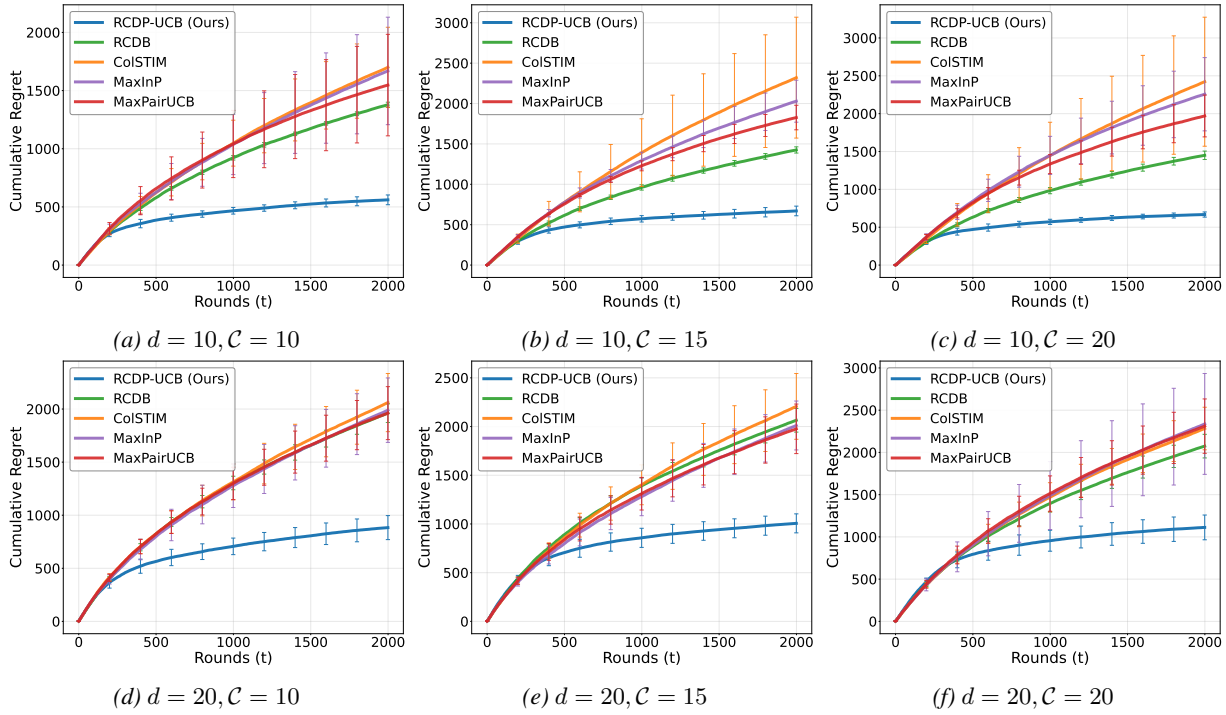


Figure E.10. **Polynomial Mapping (Varying Corruption)**: Cumulative regret with varying corruption budget C for different context dimensions ($d = 10, 20$). All experiments were conducted under fixed stochastic delay parameters ($\mu_\tau = 100, \sigma = 100$) and averaged over 5 runs.

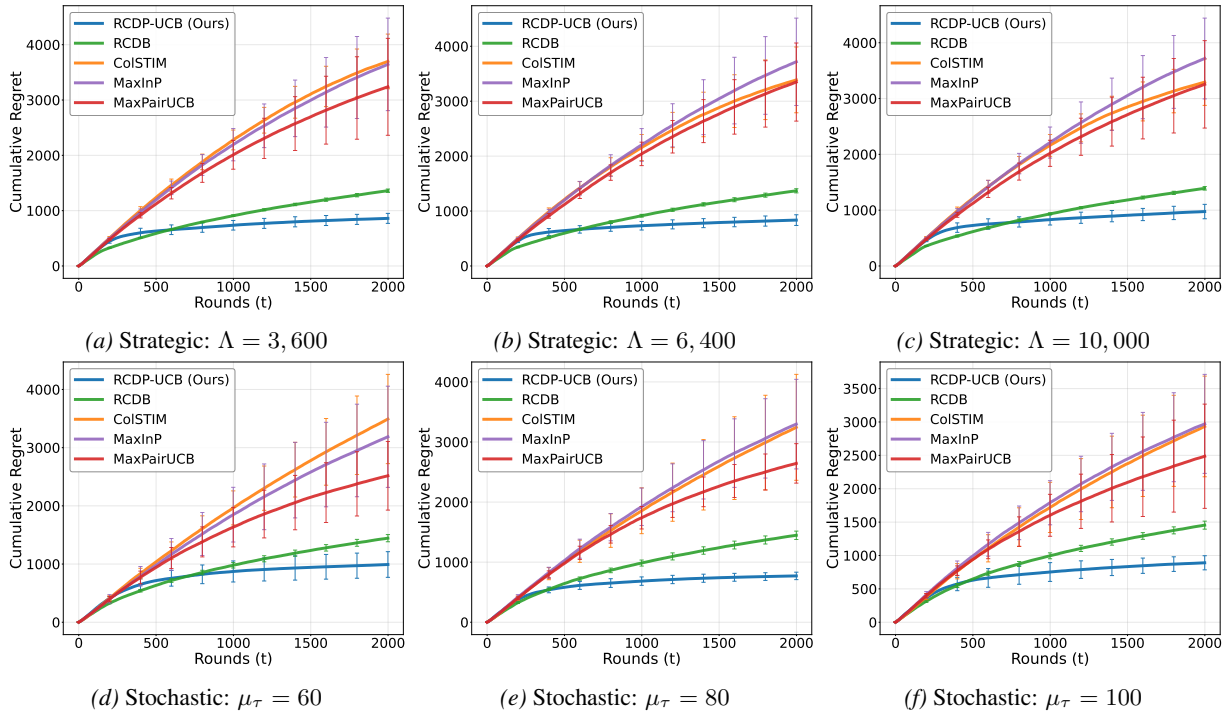


Figure E.11. **Polynomial Mapping (Pre-serving Baselines)**: Cumulative regret with varying delay budget Λ and mean delay μ_τ under adversarial corruption ($C = 25$). All experiments were conducted across 5 runs with random seeds.

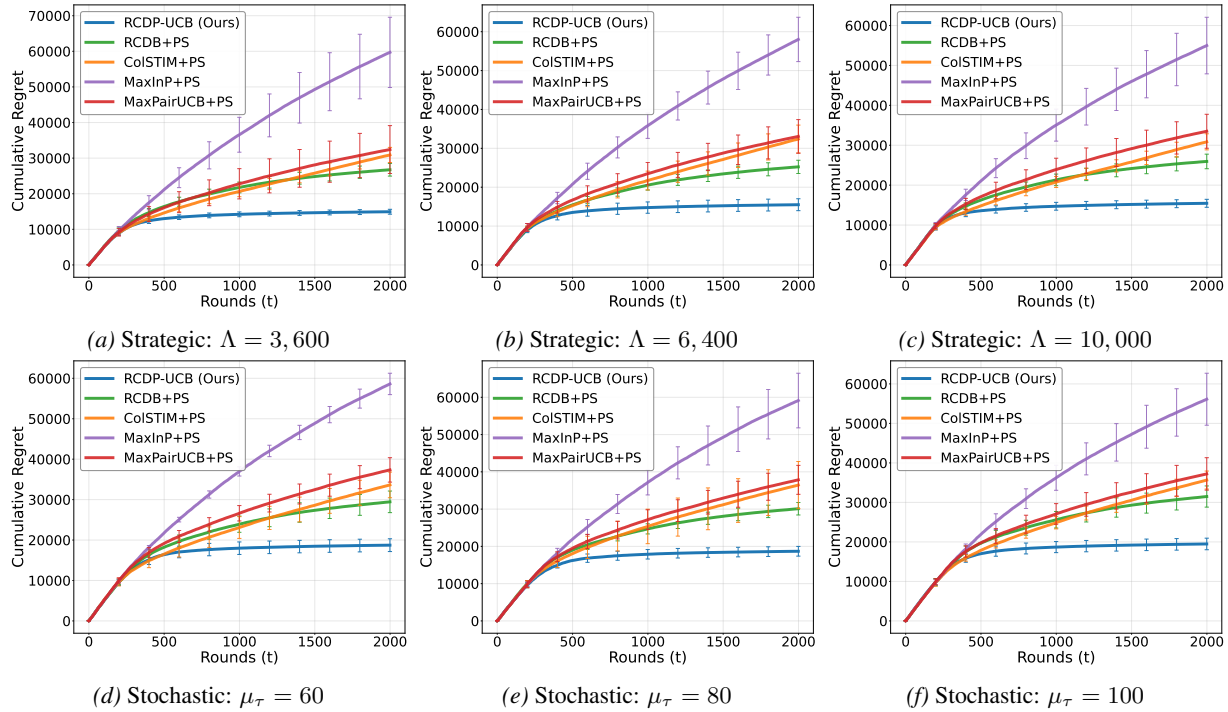


Figure E.12. **Absolute Mapping (Post-serving Learning)**: Cumulative regret with varying delay budget Λ and mean delay μ_τ under adversarial corruption ($\mathcal{C} = 25$, except $\Lambda = 10, 000$ using $\mathcal{C} = 20$). All experiments were conducted across 5 runs with random seeds.

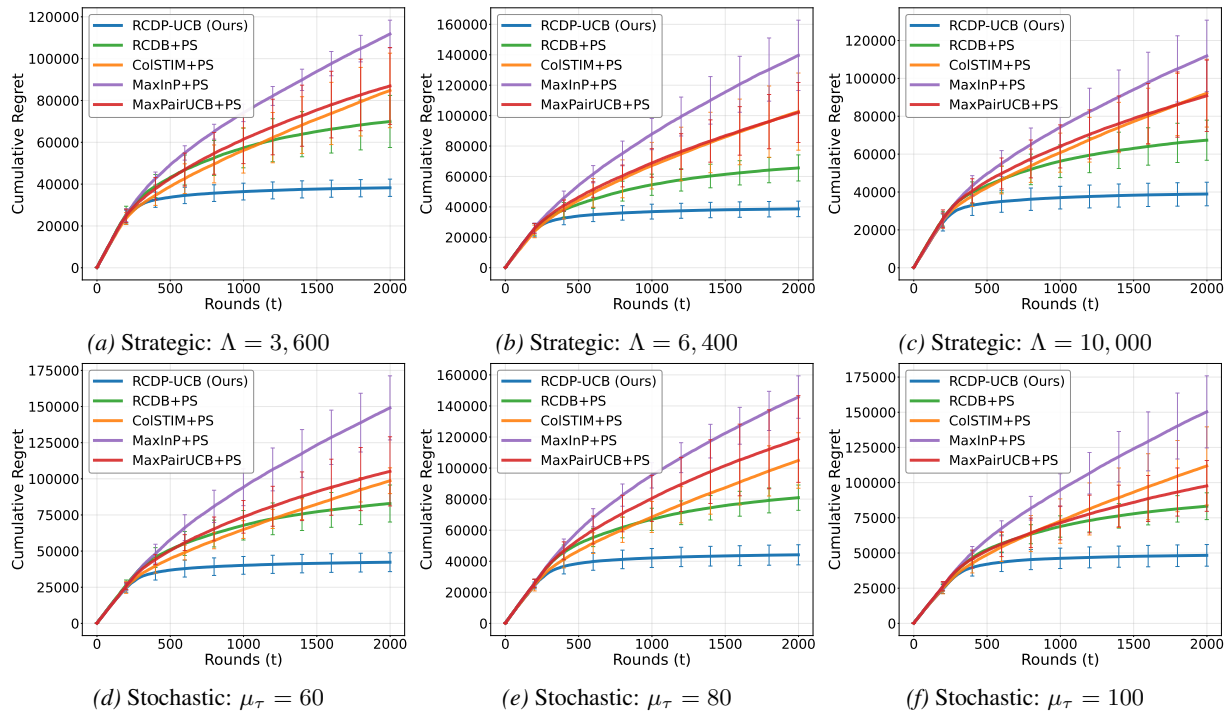


Figure E.13. **Polynomial Mapping (Post-serving Learning)**: Cumulative regret with varying delay budget Λ and mean delay μ_τ under adversarial corruption ($\mathcal{C} = 25$, except $\Lambda = 10, 000$ using $\mathcal{C} = 20$). All experiments were conducted across 5 runs with random seeds.

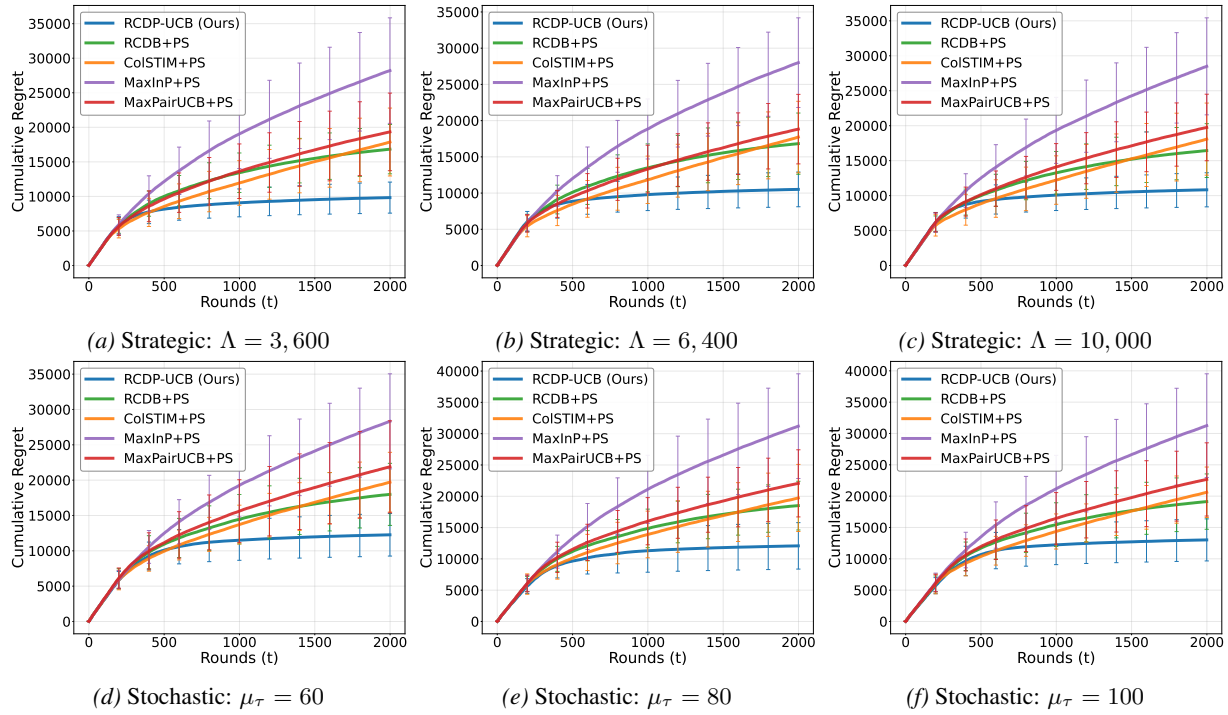


Figure E.14. **Sinusoidal Mapping (Post-serving Learning)**: Cumulative regret with varying delay budget Λ and mean delay μ_τ under adversarial corruption ($C = 25$). All experiments were conducted across 5 runs with random seeds.

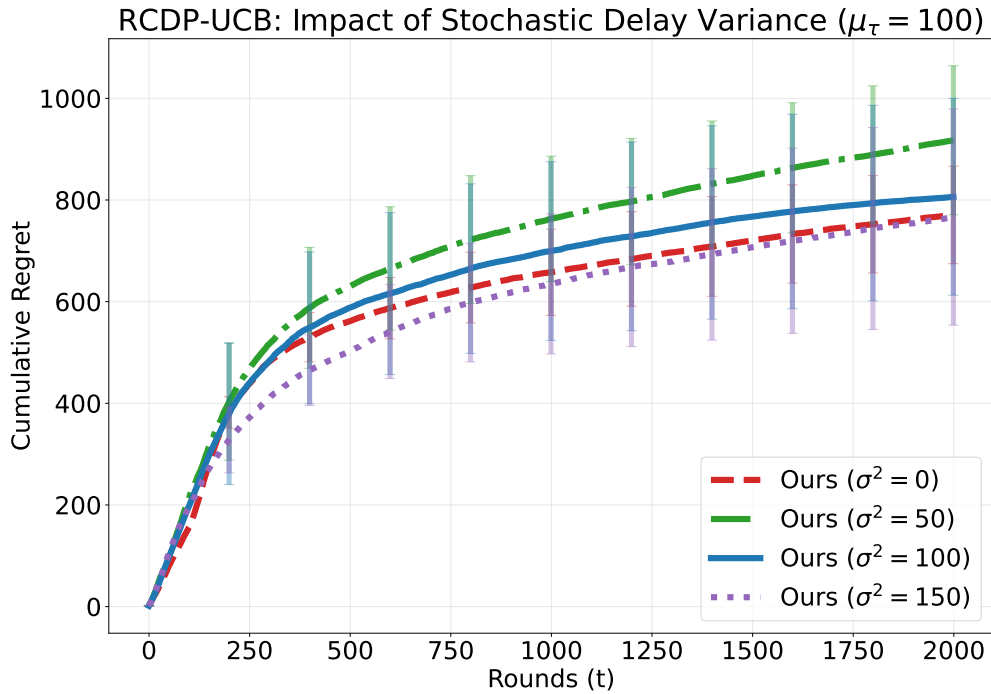


Figure E.15. **Stochastic Delay Variance Ablation**: Cumulative regret of RCDP-UCB under varying variances $\sigma^2 \in \{0, 50, 100, 150\}$ with fixed $\mu_\tau = 100$ and $C = 25$. The results are aggregated over 5 runs.